THESIS APPROVAL

GRADUATE SCHOOL, KASETSART UNIVERSITY

Master of Engineering (Chemical Engineering)

DEGREE

Chemical Engineering | Chemical Engineering

FIELD | **DEPARTMENT**

TITLE: Temperature Control of Thermal Cracking Furnace in Vinyl Chloride Monomer Process Using 2D PDEs-ODE Model

NAME: Mr. Chawin Taweerojkulsri

THIS THESIS HAS BEEN ACCEPTED BY

THESIS ADVISOR

(Assistant Professor Chanin Panjapornpon, Ph.D.)

THESIS CO-ADVISOR

(Associate Professor Apinya Duangchan, Ph.D.)

DEPARTMENT HEAD

(Associate Professor Apinya Duangchan, Ph.D.)

APPROVED BY THE GRADUATE SCHOOL ON _____

DEAN

(Associate Professor Gunjana Theeragool, D.Agr.)

THESIS

TEMPERATURE CONTROL OF THERMAL CRACKING FURNACE IN VINYL CHLORIDE MONOMER PROCESS USING 2D PDES-ODE MODEL

CHAWIN TAWEEROJKULSRI

A Thesis Submitted in Partial Fulfillment of
the Requirements for the Degree of
Master of Engineering (Chemical Engineering)
Graduate School, Kasetsart University
2014

Chawin Taweerojkulsri 2014: Temperature Control of Thermal Cracking Furnace in Vinyl Chloride Monomer Process Using 2D PDEs-ODE Model. Master of Engineering (Chemical Engineering), Major Field: Chemical Engineering, Department of Chemical Engineering. Thesis Advisor: Assistant Professor Chanin Panjapornpon, Ph.D. 71 pages.

This work presents a new control technique for the EDC thermal cracking furnace modeled by sets of ordinary differential equation (ODE) and 2D-partial differential equations (PDEs). The dynamics of coupled 2D-PDEs-ODE model are divided into 2 subsystems, set of state variables of the internal and external cracking coil. With the concept of input-output (I/O) linearization, these inner and outer dynamics are applied to design the setpoint tracking calculator and the approximate I/O feedback controller respectively. The tracking compensator and the finite-based, open-loop observer are integrated with the proposed controller system to compensate the model mismatch and predict the unmeasured state information. The performances of the proposed method are evaluated through the servo and regulatory tests. The results showed that the control method can effectively force the controlled output to the desired setpoints and reject the disturbance from changes of feed flow.

_____ _____ __ / __ / __

Student's signature Thesis Advisor's signature

ACKNOWLEDGEMENTS

It is not possible that this research will be successful without my advisor, Assistant Professor Dr. Chanin Panjapornpon. With my sincerity, I would like to say "Thank you very much" to him. He always gives advice to me when I face problems for both this research work and life.

Next, I wish to thank Associate Professor Apinya Duangchan, co-advisor, for her valuable comments and suggestions. She is so kind and gracious; I am delighted to choose her as my co-advisor.

After that, I would like to appreciate all professors, staffs, and colleagues for their recommendations and helps.

Moreover, it is indispensable for my appreciation to the Kasetsart University Research and Development Institute (KURDI), the project for Higher Education Research Promotion and National Research University Development, Office of the Higher Education Commission, and the Center of Excellence on Petrochemicals and Materials Technology (PETROMAT) for financial support to this research.

Finally, I would like to express sincere thanks to my parents for the opportunity in this study, for their supports, and for their encouragement, which makes my research succeed.

Chawin Taweerojkulsri

June 2014

TABLE OF CONTENTS

Page

LIST OF TABLES

LIST OF FIGURES

LIST OF FIGURES (Continued)

LIST OF FIGURES (Continued)

LIST OF FIGURES (Continued)

LIST OF ABBREVIATIONS

A_w	=	furnace wall area (m^2)
C_{EDC}	=	concentration of EDC (mol m^{-3})
C_{EDC}	=	concentration of VCM (mol m^{-3})
C_{p_g}	=	average heat capacity of cracked gas components ($J\ g^{-1}\ K^{-1}$)
C_{p_t}	=	heat capacity of the tube wall ($J\ g^{-1}\ K^{-1}$)
C_{p_w}	=	heat capacity of the furnace wall ($J\ g^{-1}\ K^{-1}$)
D	=	time-derivative operator
d_t	=	diameter of tube (m)
E_a	=	activation energy ($J\ mol^{-1}$)
F	=	sharp factor
ΔH	=	heat of reaction ($J\ mol^{-1}$)
ΔH_{comb}	=	heat of combustion (MJ)
h_g	=	heat transfer coefficient of mixed gases ($W\ m^{-2}\ K^{-1}$)
K	=	Kelvin
kg	=	kilogram
k_0	=	kinetic constant (s^{-1})
k_t	=	thermal conductivity of the tube wall ($W\ m^{-1}\ K^{-1}$)
k_g	=	thermal conductivity of mixed gases ($W\ m^{-1}\ K^{-1}$)
m	=	meter
$\dot{m}_{fuel}$	=	mass flow rate of the fuel gas ($kg\ s^{-1}$)
m_t	=	mass of the cracking tube (kg)
m_w	=	mass of the furnace wall (kg)
L	=	reactor length (m)
P	=	constant parameter
q	=	heat accumulation (J)
R	=	gas constant ($J\ mol^{-1}\ K^{-1}$)
r	=	coordinate
r_{EDC}	=	reaction rate (mol $m^{-3}\ s^{-1}$)

LIST OF ABBREVIATIONS (Continued)

r_{coke}	=	coke formation rate (mm month^{-1})
r_i	=	relative order of the output *i*
Re	=	Reynolds number
R_i	=	inner radius of the cracking tube (m)
R_o	=	outer radius of the cracking tube (m)
t	=	time (s)
T_g	=	gas temperature (K)
T_t	=	tube wall temperature (K)
T_{tsp}	=	setpoint of tube wall temperature (K)
T_w	=	furnace wall temperature (K)
s	=	second
u	=	manipulated input
v	=	velocity of ethylene dichloride (m s^{-1})
V	=	pipe volume
x	=	state variables
x_{ss}	=	steady-state value of the state variables
y	=	vector of the controlled outputs
y_{sp}	=	output setpoint
z	=	coordinate
ρ_g	=	density of mixed gases
y	=	vector of the controlled outputs
y_{sp}	=	output setpoint
z	=	coordinate
ρ_g	=	density of mixed gases
ρ_t	=	tube density
ρ_w	=	wall density
σ	=	Stefan- Boltzmann constant
μ	=	dynamic viscosity (N s m^{-2})
ν	=	corrected setpoint

LIST OF ABBREVIATIONS (Continued)

Φ_v	=	external energy
$\mathbb{X}$	=	vector of state variables
$\mathbb{U}$	=	vector of manipulated inputs
β_1	=	tuning parameter for the setpoint predictor
β_2	=	tuning parameter for the feedback controller
λ	=	tuning parameter for the compensator

TEMPERATURE CONTROL OF THERMAL CRACKING FURNACE IN VINYL CHLORIDE MONOMER PROCESS USING 2D PDES-ODE MODEL

INTRODUCTION

Vinyl chloride monomer (VCM) is a raw material for Poly Vinyl Chloride (PVC) production. It is typically obtained from the cracking of 1,2-dichloroethane (EDC) under 400-500°C, of which hydrogen chloride (HCl) is a byproduct. The reaction can proceed by following:

$$\underset{EDC}{C_2H_4Cl_2(g)} \rightarrow \underset{VCM}{C_2H_3Cl(g)} + \underset{Hydrogen\ Chloride}{HCl(g)}$$

The EDC cracking rate strongly depends on the reaction temperature; increase on the reaction temperature results in the high cracking rate and also the high-coking rate. The EDC vapor is reacted along the lengthy empty coil suspended in the chamber of the gas-fired cracking furnace while the formation of coke will deposit on the tube skin inside. The reaction temperature is controlled by manipulating fuel gas flow; heat occurring from burned fuel will be transferred to the tubular reactor by radiation effect. However, the occurring coke deposition will decrease the inner tube diameter and increase thermal resistance, leading to increasing on pressure drop and more required energy for maintaining a desired conversion. According to the mention above, furnace dynamics is highly nonlinear due to the spatial distributed temperature and concentration of the gas inside the cracking coil, as well as the effect of the temperature of the furnace wall. These complex behaviors and coke formation lead to deteriorating the performance of the gas temperature control by a proportional integral derivative (PID) controller. They may cause off-spec of the products, thermal runaway, plant shutdown or, in the worst case, explosion. Therefore, the control method that can handle the temperature of the cracking furnace effectively is needed to achieve a high-quality product.

There were literatures studying about the coke in EDC cracking furnace. The impurities mixed with EDC feed, such as carbon tetrachloride, molecular chlorine, and chloroprene to EDC conversion were experimented to find their effects (Incavo, (1996)). Similarly, in the Zychlinsky *et al*. (1990), the sensitivity of feed purity to EDC conversion and coke formation was studied by mixing some hydrocarbons: vinyl chloride, chloroethane, 1,1-dichloroethene, 1,2-dichloroethene, 1,1-dichloroethane, chloroform, benzene, trichloroethene, and tetrachloroethene with pure EDC feed. In 1992, Ranzi et al. developed the kinetic scheme of many elementary reactions and molecular and radical species based on general thermochemical kinetic theories by having the EDC pyrolysis system as one of the case studies to prove the reasonability of the scheme. The characterization of coke in EDC cracking furnace was found in the form of tar droplets occurred in gas-phase at the high temperature (Borsa *et al*., 1999). Moreover, they also found that the type of coke occurring in EDC cracking furnace was not the same in ethylene pyrolysis. In the next two years, the same group represented the effect of metals to the formation of coke. The results showed that the nature of coke was not changed with the effect of metals but affect to the conversion and amount of the coke formed; the coke formation rate mainly depended on % EDC conversion. For the temperature control of the furnace, the most research works only focused on the dynamics of the tubular reactor. Some works applied the model reduction technique to lump the reactor model before performing the controller synthesis. For example, the PDE was lumped by Galerkin method and then applied with infinite dimensional state feedback (Hoo and Zheng, 2001) lumped by method of characteristic and applied with robust control (Shang *et al*., 2005) and lumped by infinite dimensional method and applied with the linear, quadratic regulator (LQR) (Moghadam *et al*., 2010). Some works use the process data to develop an empirical model by the neural network method before used with a robust control (Rani and Patwardhan, 2007) or generic model control (GMC) (Aggelogiannaki and Sarimveis, 2009). Besides, there are few works considering to the interaction of wall radiation in the control of furnace. Masoumi *et al.* (2006) studied the temperature control of the naphtha thermal cracking with multi cracking coils by using the PI controller. The desired setpoints were obtained from the optimization of the temperature profile. In Zeybek (2006), the outlet gas temperature is controlled by manipulating the fuel mass

flow rate by using the adaptive heuristic controller based on three layers of feed-forward artificial network (ANN). Panjapornpon *et al.* (2012) proposed the control of coupled PDE-ODEs for EDC cracking furnace by using approximate I/O linearization; the tube temperature was controlled by manipulating the fuel gas flow while the mass production rate of VCM was handled by the PI controller by manipulating the EDC feed. The furnace model was developed by assuming a plug-flow velocity profile and neglecting the effect of the radius heat transfer. However, there are some works mentioned about significant difference of predicted process dynamics when the radial effect and velocity profile were taken into account (Van Geem *et al.*, 2004; Han *et al.*, 2007). In addition, when there is the coke formation occurring in the real process, the performance of 1D controller should be dropped, which may cause the poorer performance in the control ability. It brings about the question of the improvement of control performance when the 2D model is applied.

In this work, a new structure of the coupling 2D PDEs-ODE model for the EDC cracking furnace by using the I/O linearization is presented. The purposes of this work are to control the gas temperature at the exit tube by manipulating the fuel gas flow and predicting the thickness of coke formation with the 2D model. The dynamics of EDC cracking furnace consist of the EDC concentration and gas temperature considered as the internal states and the tube temperature and furnace wall considered as external states. PDEs describes all the dynamics except the furnace wall dynamics described by ODE. Instead of applying the I/O controller to the objective directly, the internal subsystem is used for developing the setpoint tracking calculator while the external is applied for the controller synthesis. The gas temperature is applied with I/O linearization to develop the mapping function of the equivalent tube temperature setpoint for the I/O feedback controller. The tracking compensator and the finite-based, open-loop observer are integrated into the control system to eliminate the offset and predict the unmeasured state information. For coke prediction, the average information form 2D model will be used into the coke model to calculate the coke thickness next. An advantage of proposed control method with the partitioning state dynamics is to reduce the complexity of the controller equation with a better predicting quality by using the 2D process model.

OBJECTIVES

The objective of this research is to design a model-based control system in order to control exit gas temperature by manipulating fuel gas flow with a 2D PDEs-ODE model.

Scopes of thesis

This research focuses on designing the coupling control of exit gas temperature and VCM mass flow rate. Finite-based I/O linearization is developed for coupling 2D PDEs-ODE model of the EDC cracking furnace. The developed control system composes of model-based controller impelling system to reach the goal and compensate error in the system and the developed controller can maintain stability of the process also help the prediction of the furnace lifetime for planning of turnaround period.

Impact of results

The new developed control system is an alternative for handling EDC cracking furnace. The 2D-based PDEs-ODE model which describes the furnace wall and cracking coil dynamics and controller are developed to receive more accuracy of prediction and better control performance. The more the efficient control system has, the more the safety for operation receives and the less the environment is impacted. Additionally, while the desired product quality can be maintained effectively, the operating costs will be reduced.

LITERATURE REVIEW

1. VCM production process and coke formation

Polyvinyl chloride (PVC) is widely used in many products, such as bottles, plumbing and electrical cable insulation. Vinyl chloride monomer (VCM) is an important raw material for PVC production. The physical characteristic of VCM has no color and their molecular formula and weight are C_2H_3Cl and 50.5 g/mol respectively. For VCM production, one of the important units is EDC cracker or EDC cracking furnace shown in Figure 1:

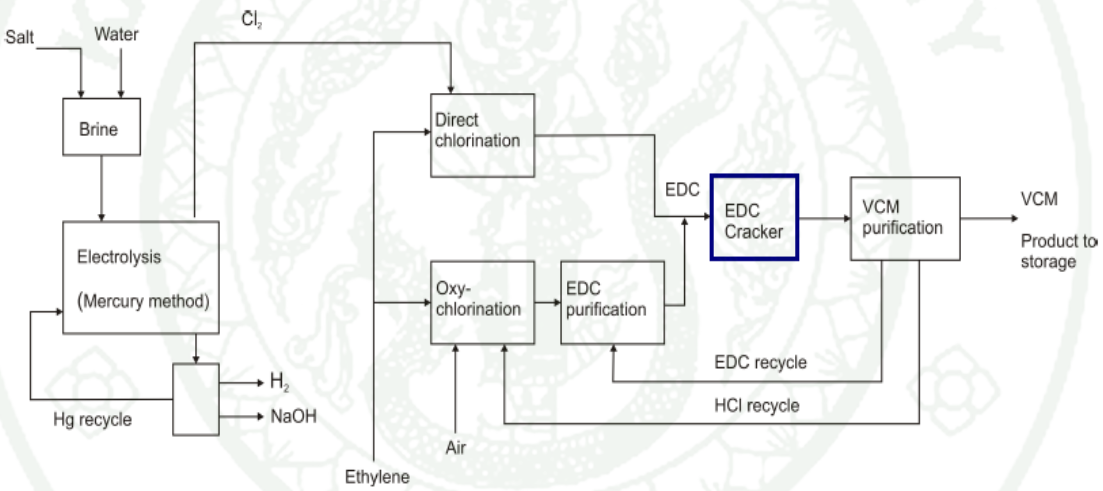

Figure 1 The VCM production block diagram

Source: Kaggerud (2007)

According to Figure 1, the EDC cracking reaction is the main reaction in producing VCM, which results from decomposing of 1,2-dichloroethane or ethylene dichloride (EDC) by having hydrogen chloride (HCl) as a byproduct as following in:

$$C_2H_4Cl_2(g) \rightarrow C_2H_3Cl(g) + HCl(g)$$

EDC *VCM* *Hydrogen Chloride*

This reaction is operated at temperature up to 500°C, pressure about 10-20 atm and 50-60% conversion of EDC and 99% selectivity of EDC formed VCM (Borsa *et al*., 2001). However, coke is one of the significant issues, affecting to several downstream parts for the VCM production, so characteristic, and causes of coke formation are also studied.

Zychlinsky *et al.* (1990) found that the EDC conversion and coke formation are very sensitive to the purity of the feed by mixing some hydrocarbons: vinyl chloride, chloroethane, 1,1-dichloroethene, 1,2-dichloroethene, 1,1-dichloroethane, chloroform, benzene, trichloroethene, and tetrachloroethene with pure EDC feed. Their results showed that the carbon tetrachloride caused the increase on both EDC conversion and coke formation; the coke formation depended on the EDC conversion resulting from EDC or EDC radical rather than CCl_4, and 50-60% of chloroprene was converted to coke.

Incavo (1996) studied the effect of impurities, such as carbon tetrachloride, molecular chlorine, and chloroprene to EDC conversion, and found that the chlorine and carbon tetrachloride affected to the increase on EDC conversion as well as the irons from the stainless steel material trended to be gas-phase catalysts.

In Ranzi *et al.* (1992), the kinetic scheme of many elementary reactions and molecular and radical species were developed, based on general thermochemical kinetic theories and know-how in hydrocarbon pyrolysis. The EDC pyrolysis system was a system used to test the scheme with the furnace model, and the coking model was also developed. The results showed reasonable values and trends and the coke occurred from vinyl chloride, acetylene, chloroprene and similar components.

Borsa *et al.* (1999) found that the characterization of coke was generated in the form of tar droplets which occurred in gas-phase at the high temperature. Such the coke would deposit on the surface of the tube in the cracking furnace. Moreover, they also found that the way to form coke between EDC cracking furnace and ethylene pyrolysis was different because many reducing procedures used in ethylene pyrolysis were proved that they could not implement in EDC cracking furnace. In the next two

years, the effect of metals to the formation of coke was studied and found that the nature of coke was not changed with the metals mixed in the feed EDC but also had an effect on the conversion and amount of the coke formed. In addition to coke deposition, the coke formation rate was mainly depended on % EDC conversion except in the case of chloride addition. It helped decrease the operating temperature and coke formation rates, but EDC conversion was lower too because of the higher of the other byproducts.

2. The controlled development of cracking furnace

In the past, most research works were interested in the dynamics of the tubular reactor only. The temperature control of cracking furnace in the part of radiation effect from the furnace wall was negligible. Some works applied the model reduction technique to lump the reactor model before performing the controller synthesis. The first-order hyperbolic PDE was applied to control the tubular reactor. Shang *et al*., (2005) applied the robust control from the PDE lumped by the method of characteristic. The control law was developed in order that the closed-loop response of the process output moved towards the desired setpoint along the characteristic curve. Hoo and Zheng (2001) developed the infinite dimensional state feedback from the PDE lumped by Galerkin method. One-dimensional partial differential was used as two case studies. Such models were approximated in the form of the low-order model to develop the state feedback controllers. The controller performance of them was satisfied under the ideal and non-ideal conditions when the nonlinear controller output was more initially aggressive. Additionally, the accuracy of the low-order model was important to the control performance. Moghadam *et al.* (2010) developed the linear quadratic regulator (LQR) from the PDE lumped by infinite dimensional method to control the output. The proposed control method gave the successful result for forcing the output at the desired setpoint, but the model transformation of this method was very difficult. For the empirical model, the process data was used before applied the controller techniques. Aggeologiannaki and Sarimveis (2009) used the data from the process for developing the neural network with radial basis function (RBF) to identify the hyperbolic distributed parameter systems (DPSs). The robust H_∞ control law was

used to apply the temperature distribution for a long duct for the flow-based control. The proposed control method demonstrated a good performance; the quality of the controller depended on the empirical model. Besides, there are few works considering to the interaction of wall radiation in the control of furnace. Masoumi *et al.* (2006) studied the temperature control of the naphtha thermal cracking with multi cracking coils by using the PI controller. The desired setpoints were obtained from the optimization of the temperature profile. However, using this method had to face the difficult selecting for tuning parameters and the narrow range of operation which did not cover the closed-loop stability along the operating region. Zeybek (2006) developed the control method which considered the effects of the furnace wall and cracking coil dynamics. The outlet gas temperature is controlled by manipulating the fuel mass flow rate by using the adaptive heuristic controller based on three layers of feed-forward artificial network (ANN). This control method was attractive for implementation in industrial, but the robustness control for the feed flow changed in operation was not reported. However, in 2012, Panjapornpon *et al.* proposed the control of coupled PDE-ODEs for EDC cracking furnace by using approximate I/O linearization; the dynamics of cracking coil and furnace wall was considered. The furnace model was developed by assuming a plug-flow velocity profile and neglecting the effect of the radius heat transfer. The tube temperature was controlled by manipulating the fuel gas flow while the mass production rate of VCM was handled by the PI controller by manipulating the EDC feed.

3. Input/Output (I/O) linearization technique

The ideal of linerizing only part of the dynamics, i.e. the dynamics between the input and output, has been widely used. In such a scheme, referred to as input/output linearization, the nonlinearities are pushed to the so-called internal dynamics. In the context of input-output linearization, the main consideration is that the internal dynamics should be stable.

Input-Output linearization is a controller synthesis technique that involves coordinating transformation to construct a relationship between the original system output, y, and the new input, ν, in a linear form.

Consider the continuous-time multivariable nonlinear system in a compact form:

$$\begin{aligned} \dot{x} &= f(x,u) \\ y &= h(x) \end{aligned} \tag{1}$$

where $x(t) = [x_1, \ldots, x_n]^T \in \mathbb{X}$ is the vector of state variables, $u = [u_1, \ldots, u_m]^T \in \mathbb{U}$ is the vector of manipulated inputs, $f(x,u)$ is a nonlinear vector function, and $y = [y_1, \ldots, y_m]^T$ is the vector of controlled outputs.

The responses of the closed-loop process output are requested, having the linear form:

$$\begin{aligned} (\beta_1 D + 1)^{r_1} y_1 &= y_{sp_1} \\ &\vdots \\ (\beta_m D + 1)^{r_m} y_m &= y_{sp_m} \end{aligned} \tag{2}$$

where D is the differential operator (i.e., $D \triangleq d/dt$), $\beta_1, \ldots, \beta_m$ are positive, constant parameters that set the speed of the closed-loop response of outputs $y_1, \ldots, y_m$ respectively, and $y_{sp_1}, \ldots, y_{sp_m}$ are the output setpoints. The relative order of the controlled output y_i is denoted by r_i, where r_i is the smallest integer for which $(\partial / \partial u_i)\left(d^{r_i} y_i / dt^{r_i}\right) \neq 0$. The following notation is used:

$$
\begin{aligned}
y_i &= h_i^0(x) \\
\frac{dy_i}{dt} &= h_i^1(x) \\
\frac{d^2 y_i}{dt^2} &= h_i^2(x) \\
&\vdots \\
\frac{d^{r_i-1} y_i}{dt^{r_i-1}} &= h_i^{r_i-1}(x) \\
\frac{d^{r_i} y_i}{dt^{r_i}} &= h_i^{r_i}(x, u_i)
\end{aligned}
\tag{3}
$$

This notation is made based on the following assumptions:

1) The relative order $r_1, \ldots, r_m$ are finite.

2) The characteristic matrix of the process, $\partial h_i^{r_i}(x, u_i)/\partial u_i \neq [0 \ldots 0]$, is non-singular on $\mathbb{X} \times \mathbb{U}$.

3) The process is controllable and observable locally around the nominal steady state.

4) The matrices $\partial f / \partial x$ and $(\partial h / \partial x)(\partial f / \partial x)^{-1}(\partial f / \partial u)$ evaluated at nominal steady state pair, (x_{ss}, u_{ss}), are non-singular.

In the case that the controlled output, y, does not have a finite relative order, $r = \infty$, the manipulated input, u, does not affect the controlled output. The feedback controller is obtained by solving the equation (2). The compact form of the feedback controller denotes by:

$$
u_i = \psi(x, y_{sp_i}) \tag{4}
$$

4. Computational fluid dynamics (CFD) technique

The tubular reactor models were typically applied with reduction techniques before synthesizing controllers. For physical control, PDE equations were lumped by Galerkin method, method of characteristic and infinite dimensional method, and applied with infinite dimensional state feedback (Hoo and Zheng, 2001), robust control (Shang *et al*., 2005) and the linear quadratic regulator (LQR) (Moghadam *et al*., 2010), respectively. For the empirical model, the process data was used to develop neural network method before implemented with a robust control (Rani and Patwardhan, 2007) or generic model control (GMC) (Aggelogiannaki and Sarimveis, 2009). However, the reduction techniques may not be suitable to describe the fluid behaviors, so computational fluid dynamics (CFD) is an attractive alternative of engineering tool for predicting the flow and temperature fields (Bernard *et al*., 2005). Therefore, there have been a lot of CFD implemented in chemical process, for examples, Nijemeisland and Dixon (2001) did an excellent review of these computational treatments of which CFD approach was used to solve the Navier-Stokes equations and the energy balance over control volumes depended on both spatial coordinate and time, and in the modeling of CPU heat sink, a real-coded genetic algorithm was used to find an optimal set of plate-fin shape parameters instead of using the finite element method to receive a better of heat dispersion performance for the investigation of heat transfer phenomena (Chen *et al*., 2008).

MATERIALS AND METHODS

Materials

1. Personal Computer with Intel(R) Core(TM) i7-3930K CPU at 3.20 GHz and RAM 32.0 GB running on Microsoft Windows 7 Professional x64 Edition
2. Software
   2.1 MATLAB Version R2013a (The Math Works, Inc.)
   2.2 COMSOL 4.3 (COMSOL, Inc.)
   2.3 MATHEMATICA version 9.0 (wolfram Research, Inc.)

Methods

This research develops the control system of 2D-PDE-ODE model for EDC cracking furnace. The procedure is divided into four steps shown in Figure 2. The first step is to develop the mathematical model of EDC cracking furnace which is the coupling of PDEs and ODE. Such the equations are used to describe the cracking coil and furnace wall dynamics. Then, the I/O linearizing controller, setpoint tracking, open-loop observer, compensator and feedback controller calculator are implemented in each developed structure to confirm the closed-loop stability and eliminate the process mismatch as well as unmeasured disturbances. The control system performance is simulated by COMSOL, and the servo and regulatory tests are used to measure the controller performance by the following steps shown in Figure 2.

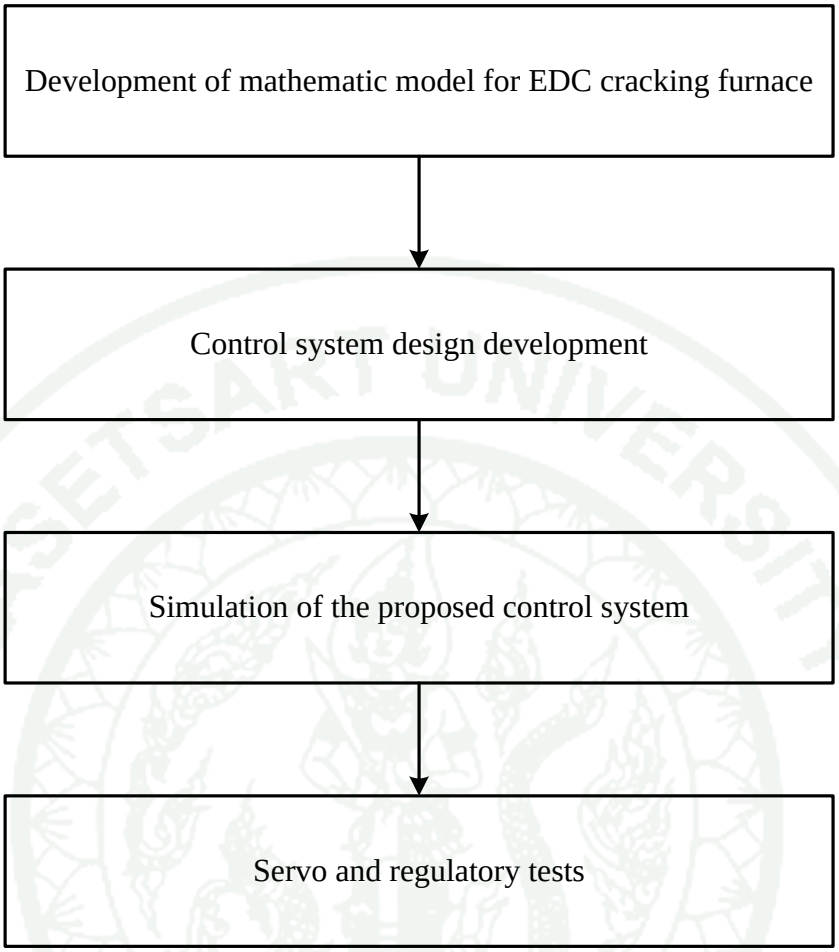

Figure 2 Control system development procedure for EDC cracking furnace

1. Development of the mathematic model of EDC cracking furnace

For this work, the state dynamics used to explain the EDC cracking furnace are the dynamics of EDC concentration, gas temperature, tube temperature and furnace wall temperature. The EDC concentration, gas temperature, and tube temperature dynamics depend on spatial coordinate and time, while the dynamic of furnace wall temperature is a function of time only. All of the dynamics are developed from reduction of mass and energy balance equations in cylindrical coordinate (James *et al.* 2007):

Mass balance:

$$\frac{\partial C}{\partial t}+v_r\frac{\partial C}{\partial t}+\frac{v_\theta}{r}\frac{\partial C}{\partial \theta}+v_z\frac{\partial C}{\partial z}=D_{AB}[\frac{1}{r}\frac{\partial}{\partial r}(r\frac{\partial C}{\partial r})+\frac{1}{r^2}\frac{\partial^2 C}{\partial \theta^2}+\frac{\partial^2 C}{\partial z^2}] \quad (5)$$

Energy balance:

$$\rho c_p\frac{DT}{Dt}=k\left(\frac{1}{r}\frac{\partial}{\partial r}\left(r\frac{\partial T}{\partial r}\right)+\frac{1}{r^2}\frac{\partial^2 T}{\partial \theta^2}+\frac{\partial^2 T}{\partial z^2}\right)+\Phi_v \quad (6)$$

where Φ_v is the external energy or the heat of reaction.

2. Control system design development

The model of the fired-furnace in Equations (18)-(22) described by partial differential equations in *r* and *z* coordinates and ordinary differential equation can be grouped into two subsystems.

The subsystem of Equation (7) expresses the interaction of the state variables inside the cracking coil and the subsystem in Equation 8 expresses the interaction of the state variables outside the cracking coil and the radiating wall.

$$\frac{\partial x_{p1}(r,z,t)}{\partial t}=-a\frac{\partial x_{p1}}{\partial z}+b\frac{1}{r}\frac{\partial}{\partial r}\left(r\cdot\frac{\partial x_{p1}}{\partial r}\right)+M(x_{p1},x_{p2}) \quad (7)$$

$$\begin{aligned}\frac{\partial x_{p2}(z,t)}{\partial t}&=c\frac{\partial^2 x_{p2}}{\partial z^2}+N(x_{p1},x_o(t))+O(x_{p2},x_o)\\ \frac{dx_o(t)}{dt}&=f(x_o,x_{p2},u(t))\\ y&=h(x_{p1})\end{aligned} \quad (8)$$

with the initial and boundary conditions of Equation (7):

$$B.C.\begin{cases}\dfrac{\partial x_{p1}(0,z,t)}{\partial r}=0\\ x_{p1}(R,z,t)=x_{p2}(z,t) \text{ or } \dfrac{\partial x_{p1}(R,z,t)}{\partial r}=0\\ x_{p1}(r,0,t)=x_{p1}(r,t)\end{cases}$$

$$I.C. \qquad x_{p1}(r,z,0)=x_{p1,0}(r,z)$$

and the initial and boundary conditions of Equation (8):

$$B.C.\begin{cases} x_{p2}(0,t)=x_{p2}(t)\\ \left.\dfrac{\partial x_{p2}}{\partial z}\right|_{z=L}=0\end{cases}$$

$$I.C.\begin{cases} x_{p2}(z,0)=x_{p2,0}(z)\\ x_o(t=0)=x_{o,0}\end{cases}$$

Where $x_{p1}(r,z,t)$ denotes the vector of the state variables depending on r and z coordinates, denotes the state variable of the external tube dynamics which is directly affected by x_o, $x_o(t)$ denote the state variable which depend on time, y denote the output variable, $z \in [0,L]$ and $r \in [0,R_o]$ are spatial coordinates, $t \in [0,\infty]$ is the time, and $u(t)$ is the manipulated variable.

In our case, the process model is highly complex due to coupled PDEs and ODE. The control objective is to regulate the output at the exit of the tube ($y=L$), the state in the subsystem Equation (7), by adjusting the input (u) in the subsystem Equation (8). To reduce complexity of the controller design, in this work, the set of PDE in Equation (7) described the internal tube dynamics will be used to create a tracking relation between the output (y) and the distributed state variable related to the lumped dynamics (x_{p2}). The set of coupling PDEs-ODE in Equation (8) described the external tube dynamics will be used to develop the I/O feedback controller that the control action (u) is obtained by solving closed-loop response of x_{p2}.

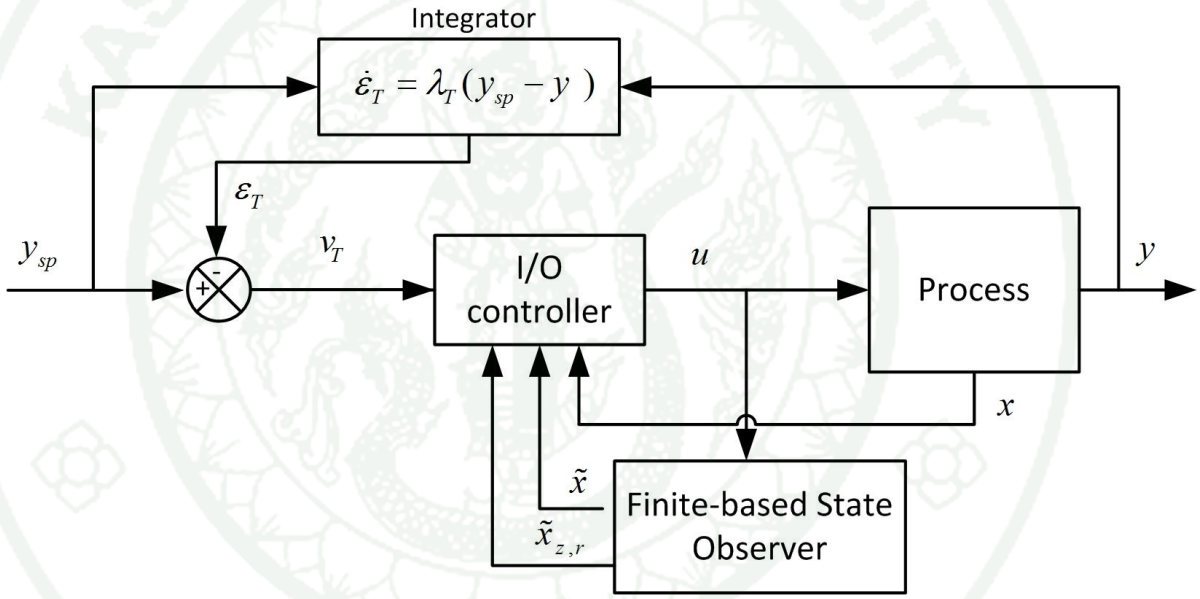

Figure 3 Schematic diagram of the controller structure 1

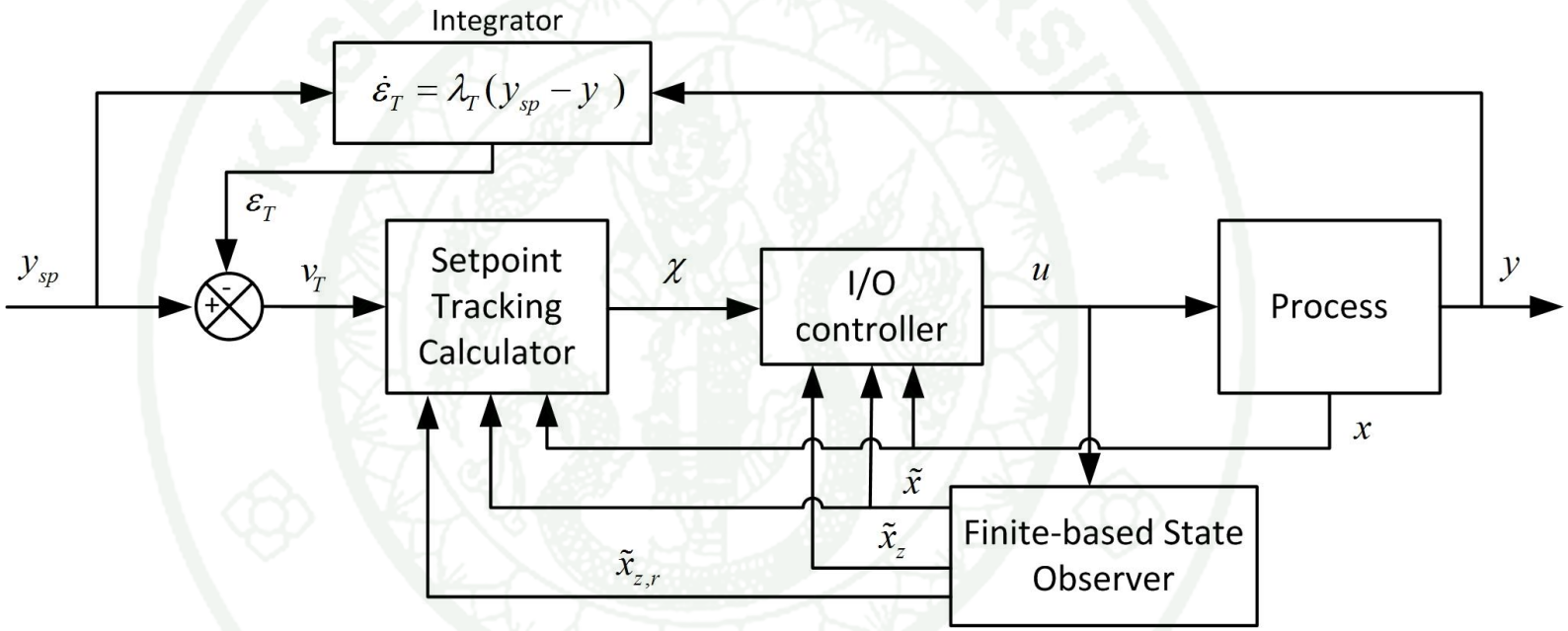

Figure 4 Schematic diagram of the controller structure 2

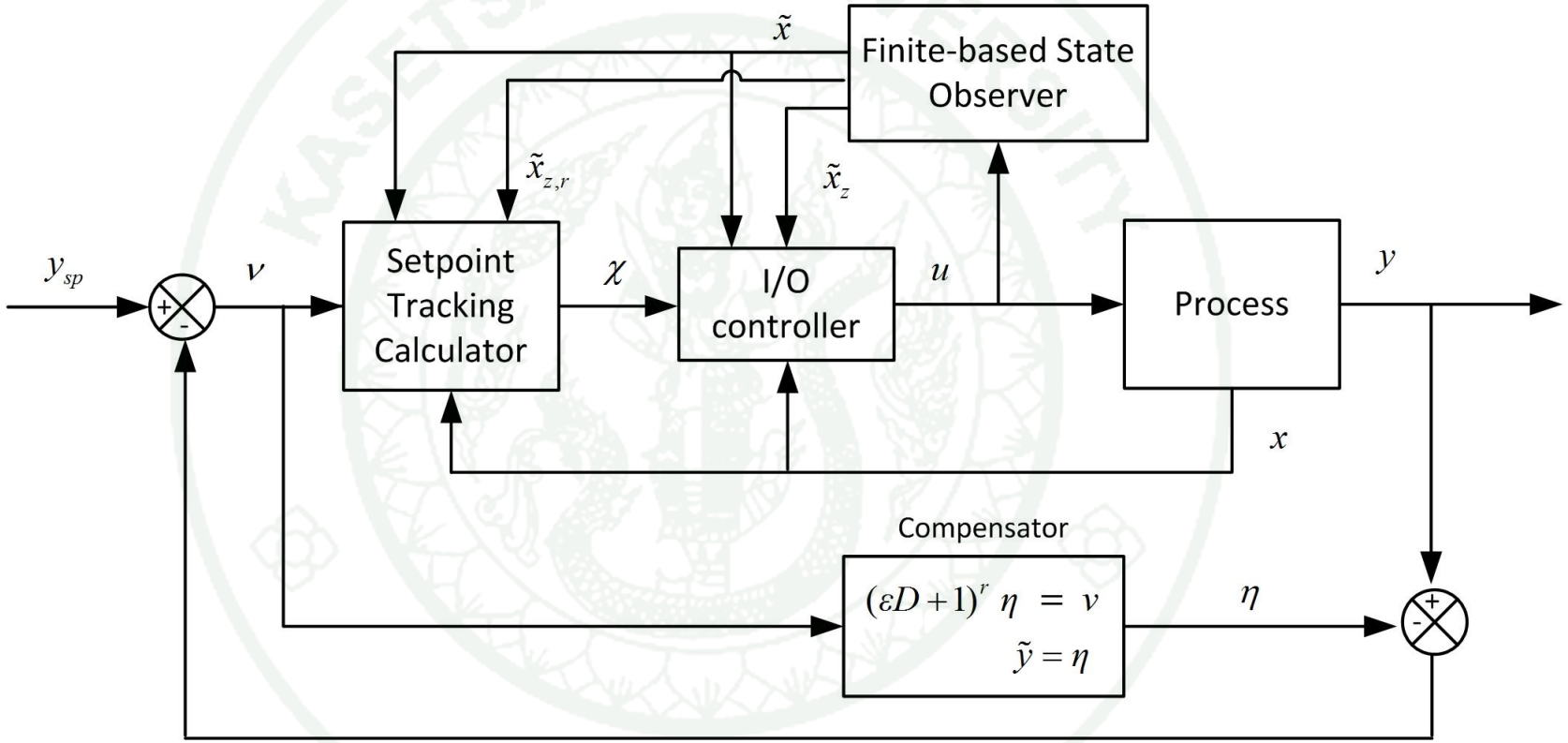

Figure 5 Schematic diagram of the controller structure 3

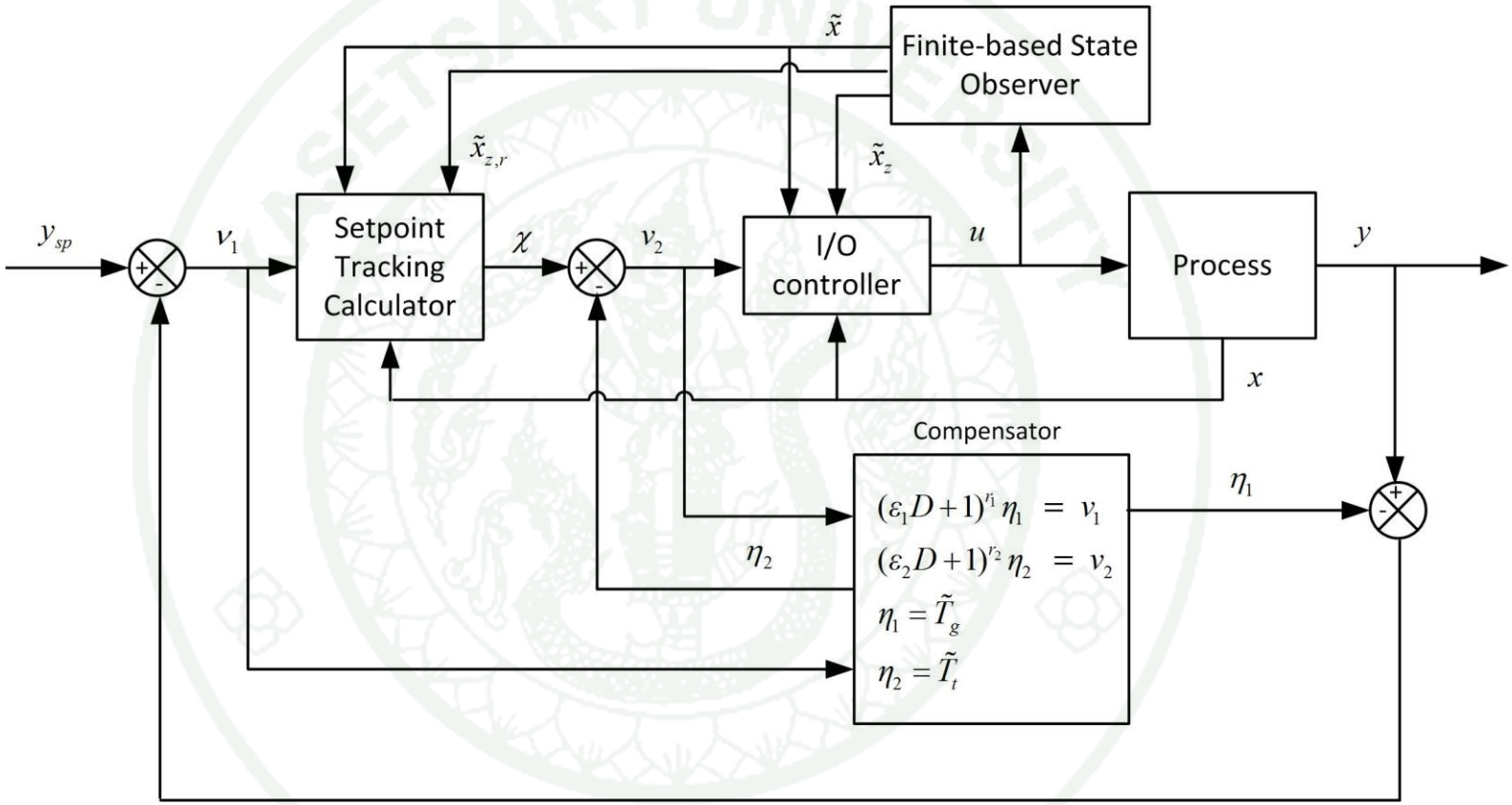

Figure 6 Schematic diagram of the controller structure 4

For this system, the proposed control is developed in sequential steps shown by the schematic diagram of the control system in Figures 3-6 above. The control system consists of a setpoint tracking calculator, I/O linearizing controller, and a finite-based, open-loop observer. More details of the control system design are given as follows.

2.1 Setpoint tracking calculator

The input/output linearization is a method that creates a linear relationship between input and output based on the coordinate transformation. It is traditionally applied for the ODE system. For the application of PDEs-ODEs system, let consider the system in Equation (9).

$$\begin{aligned} \frac{d\bar{x}}{dt} &= f(\bar{x}, \bar{x}_r, \bar{x}_{rr}, \bar{x}_z, \bar{x}_{zz}, \bar{u}) \\ \bar{y}_L &= h(\bar{x})\big|_{r=0,z=L} \end{aligned} \tag{9}$$

where $\bar{x}$ is the vector of state variables, $\bar{x}_z = \partial\bar{x}/\partial z$ and $\bar{x}_r = \partial\bar{x}/\partial r$ are the first-order spatial derivatives of $\bar{x}$ respect to *z*-direction and *r*-directions, $\bar{x}_{zz} = \partial^2\bar{x}/\partial z^2$ and $\bar{x}_{rr} = \partial^2\bar{x}/\partial r^2$ are the second-order spatial derivatives of $\bar{x}$ respect to *z*-direction and *r*-direction, $\bar{u}$ is the manipulated input and *h* is the vector of nonlinear functions. The relative order of the controlled output y_L, r, can be defined by following notation:

$$y_L = h\,(\bar{x})\big|_{r=0,z=L}$$

$$\frac{dy_L}{dt} \triangleq \left[\frac{h}{\partial\bar{x}}\frac{\partial\bar{x}}{\partial t}\right]_{z=L} = h^1\left(\bar{x}, \bar{x}_r, \bar{x}_{rr}, \bar{x}_z, \bar{x}_{zz}\right)\Big|_{r=0,z=L}$$

$$\vdots$$

$$\frac{d^{r-1}y_L}{dt^{r-1}} \triangleq \left[\begin{array}{l}\dfrac{\partial h^{r-2}}{\partial\bar{x}}\dfrac{\partial\bar{x}}{\partial t} + \dfrac{\partial h^{r-2}}{\partial\bar{x}_r}\dfrac{\partial\bar{x}_r}{\partial t} + \dfrac{\partial h^{r-2}}{\partial\bar{x}_{rr}}\dfrac{\partial\bar{x}_{rr}}{\partial t} \\ + \dfrac{\partial h^{r-2}}{\partial\bar{x}_z}\dfrac{\partial\bar{x}_z}{\partial t} + \dfrac{\partial h^{r-2}}{\partial\bar{x}_{zz}}\dfrac{\partial\bar{x}_{zz}}{\partial t} + \ldots + \dfrac{\partial^{r-2}}{\partial t^{r-2}}(\bar{x}_{zz})\end{array}\right]_{r=0,z=L}$$

$$= h^{r-1}\left(\begin{array}{l}\bar{x}, \bar{x}_r, \bar{x}_{rr}, \bar{x}_z, \bar{x}_{zz}, \dfrac{\partial\bar{x}_r}{\partial t}, \ldots, \dfrac{\partial^{r-2}}{\partial t^{r-2}}(\bar{x}_r), \dfrac{\partial\bar{x}_{rr}}{\partial t}, \ldots, \\ \dfrac{\partial^{r-2}}{\partial t^{r-2}}(\bar{x}_{rr}), \dfrac{\partial\bar{x}_z}{\partial t}, \ldots, \dfrac{\partial^{r-2}}{\partial t^{r-2}}(\bar{x}_z), \dfrac{\partial\bar{x}_{zz}}{\partial t}, \ldots, \dfrac{\partial^{r-2}}{\partial t^{r-2}}(\bar{x}_{zz})\end{array}\right)\Bigg|_{r=0,z=L}$$

$$\frac{d^r y_L}{dt^r} \triangleq \left[\begin{array}{l}\dfrac{\partial h^{r-1}}{\partial\bar{x}}\dfrac{\partial\bar{x}}{\partial t} + \dfrac{\partial h^{r-1}}{\partial\bar{x}_r}\dfrac{\partial\bar{x}_r}{\partial t} + \dfrac{\partial h^{r-1}}{\partial\bar{x}_{rr}}\dfrac{\partial\bar{x}_{rr}}{\partial t} \\ + \dfrac{\partial h^{r-1}}{\partial\bar{x}_z}\dfrac{\partial\bar{x}_z}{\partial t} + \dfrac{\partial h^{r-1}}{\partial\bar{x}_{zz}}\dfrac{\partial\bar{x}_{zz}}{\partial t} + \ldots + \dfrac{\partial^{r-1}}{\partial t^{r-1}}(\bar{x}_{zz})\end{array}\right]_{r=0,z=L}$$

$$= h^{r}\left(\begin{array}{l}\bar{x}, \bar{x}_r, \bar{x}_{rr}, \bar{x}_z, \bar{x}_{zz}, \dfrac{\partial\bar{x}_r}{\partial t}, \ldots, \dfrac{\partial^{r-1}}{\partial t^{r-1}}(\bar{x}_r), \dfrac{\partial\bar{x}_{rr}}{\partial t}, \ldots, \\ \dfrac{\partial^{r-1}}{\partial t^{r-1}}(\bar{x}_{rr}), \dfrac{\partial\bar{x}_z}{\partial t}, \ldots, \dfrac{\partial^{r-1}}{\partial t^{r-1}}(\bar{x}_z), \dfrac{\partial\bar{x}_{zz}}{\partial t}, \ldots, \dfrac{\partial^{r-1}}{\partial t^{r-1}}(\bar{x}_{zz}), \bar{u}\end{array}\right)\Bigg|_{r=0,z=L} \tag{10}$$

The setpoint tracking calculator is applied to develop a correlation between $y - x_{p2}$. From the subsystem in Equation (7), the closed-loop response of the output at the center of the exit tube is in linear form as follows:

$$\left(\beta_1\mathcal{D}+1\right)^{r_1} y_L = y_{L,sp} \tag{11}$$

where $\mathcal{D}$ is the differential operator, y_L is the output at a position $r = 0$ and $z = L$, $y_{L,sp}$ is the desired setpoint, β_1 is the tuning parameter used to adjust the speed of the output response and r_1 is the relative order of y_L with respect to x_{p2}.

By substituting the time derivatives of Equation (10) into Equation (11) and setting all time derivatives of the state gradients to be zero, the closed-loop responses of the output can be presented in a compact form

$$\phi_T(x_{p1}, x_{p1,r}, x_{p1,rr}, x_{p1,z}, x_{p2}) = y_{L,sp} \tag{12}$$

the tracking setpoint function (χ) of can be obtained by solving Equation (12) for x_{p2}, in following form:

$$\chi = \psi_T(x_{p1}, x_{p1,r}, x_{p1,rr}, x_{p1,z}, x_{p2}, y_{L,sp}) \tag{13}$$

2.2 Feedback I/O linearizing controller

From the subsystem in Equation (8), the closed-loop responses of the state x_{p2} at the position $z = L$ are requested in linear form as follows:

$$(\beta_2 \mathcal{D} + 1)^{r_2} x_{p2} = \chi \tag{14}$$

where ν is the tracking setpoint function, β_2 is the tuning parameter and r_2 is the relative order of x_{p2} with respect to u.

We substitute the time derivative in Equation (10) into Equation (14) and set all time derivatives of the state gradients to be zero. The closed-loop responses of the state x_{p2} can be presented in a compact form

$$\phi_T(x_{p1}, x_{p2}, x_{zz}, u) = \chi \tag{15}$$

Thus, the feedback controller (u) is obtained by solving Equation (15). The compact form of the controller equation is denoted by Equation (16)

$$u = \Psi(x_{p1}, x_{p2}, x_{zz}, \chi) \tag{16}$$

2.3 Finite-based state observer

The CFD technique is a useful tool to predict behavior of the system of the complex PDE problem by using the numerical calculation. Thus, in this work, a CFD-based, open-loop state observer is developed to provide the estimation of the unmeasured process concentration, $\tilde{C}$, and the state derivatives.

2.4 Integrator

In this work, there are two types of integrators used for compensating the process-model mismatch and the error from the estimate states; the controller in Equation (16) is applied with the first-order error dynamics:

$$\begin{aligned} \dot{\varepsilon}_T &= \lambda_T \left(y_{sp} - y\right)\big|_{r=0,z=L} \\ v_T &= y_{sp} - \varepsilon_T \end{aligned} \tag{17}$$

where ε_T is the output error, λ_T is a positive parameter, and v_T is the corrected setpoint, and the tracking compensator:

$$\begin{aligned} (\varepsilon D + 1)^r \eta &= v \\ \eta &= \tilde{y} \end{aligned} \tag{18}$$

where $\mathcal{D}$ is the differential operator, η is the output tracking at the position $r = 0$ and $z = L$, ε is the tuning parameter used to adjust the speed of the output tracking, and r is the relative order of the controller used this compensator.

3. Simulation of the proposed control system

The feedback controller equations were solved by MATHEMATICA software before simulated by using MATLAB and COMSOL software. The unmeasured process and the state derivatives were solved by COMSOL software.

4. Servo and regulatory tests

The proposed control method is tested with servo and regulatory to ensure the performance of the developed control system. For servo performance, the input setpoint is changed to the new value after the output response approaches the required setpoint while regulatory performance is tested by introducing the disturbance to the process after the output response approaches the required setpoint.

RESULTS AND DISCUSSION

In this section, the results are divided into three parts; the first is mathematic model of EDC cracking furnace, the second is the controller performance with servo and regulatory tests and the last is the comparison of purposed control system with the 1D controller.

1. Mathematic model of EDC cracking furnace

A simple process scheme of an EDC cracking furnace is shown in Figure 7. In the operation, EDC vapor is fed to the cracking coil and converted to VCM and HCl. The natural gas is used as a combustion fuel to supply the energy to the furnace to rise the furnace wall temperature (T_w). The furnace wall radiates and transfers the energy to the tube inside leading to the change of the tube temperature (T_t), the gas temperature (T_g) and EDC concentration (C_{EDC}) consequently.

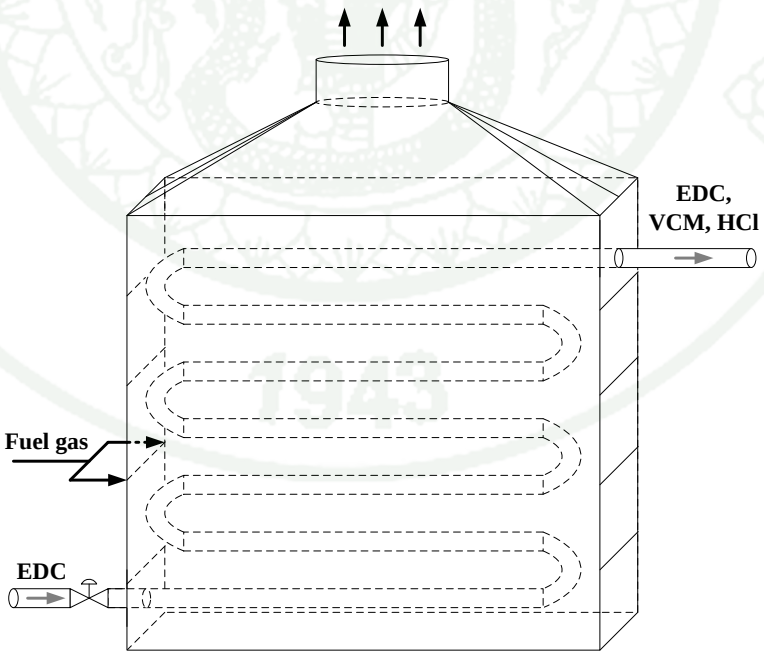

Figure 7 EDC cracking furnace

In this work, the proposed control strategy is applied with 2D PDEs-ODE model of EDC cracking furnace. The following model assumptions are applied:

Assumptions

1) All gases in the system are ideal.

2) Only the heat of reaction in $C_2H_4Cl_2(g) \rightarrow C_2H_3Cl(g) + HCl(g)$ is considered for the change of gas temperature.

3) Neglect effects of all elbows and fittings; straight tube is assumed.

4) The properties of gases in the tube are constant: k_g, ρ_g and C_{pg} .

5) The tube temperature is varied along the z-direction only because of the pipe thickness << the coil distance.

6) The gas temperature and EDC concentration are varied in both the radius and distance of the coil.

The dynamic models of the cracking furnace are represented by following equations

- The dynamics of EDC concentration and reactor temperature in the cracking coil:

$$\frac{\partial C_{EDC}}{\partial t} = -v\frac{\partial C_{EDC}}{\partial z} + \frac{k_g}{\rho_g C_{pg}}\frac{1}{r}\frac{\partial}{\partial r}\left(r\frac{\partial C_{EDC}}{\partial r}\right) + r_{EDC}$$

$$\frac{\partial T_g}{\partial t} = -v\frac{\partial T_g}{\partial z} + \frac{k_g}{\rho_g C_{pg}}\frac{1}{r}\frac{\partial}{\partial r}\left(r\frac{\partial T_g}{\partial r}\right) + \frac{A_t F\sigma}{V_t \rho_g C_{pg}}(T_t^4 - T_g^4) + \frac{|r_{EDC}^{'''}|(\Delta H)_{EDC}}{\rho_g C_{p_g}} \qquad (18)$$

$$r_{EDC} = -k_0 e^{-\frac{E_a}{RT_g}} C_{EDC}$$

with the following boundary and initial conditions:

for the EDC concentration,

$$B.C.\begin{cases} \dfrac{\partial C_{EDC}}{\partial r}(0,z,t)=0 \\ \dfrac{\partial C_{EDC}}{\partial r}(R_i,z,t)=0 \\ C_{EDC}(r,0,t)=C_{EDC,0} \end{cases} \qquad I.C.\quad x_{p1}(r,z,0)=x_{p1,0}(r,z)$$

and for the gas temperature,

$$B.C.\begin{cases} \dfrac{\partial T_g}{\partial r}(0,z,t)=0 \\ T_g(R_i,z,t)=T_t(z,t) \\ T_g(r,0,t)=T_{g,0} \end{cases} \qquad I.C.\quad T_g(r,z,t=0)=T_{g,0}$$

The velocity profile describing gas flowing was referred from an empirical/analytical solution of turbulence model in Mercado and Nunhez (2000):

$$v(r)=12.85\sqrt{\frac{-dP/dz\cdot R_i}{2\cdot\rho_g}}+\sqrt{\frac{-dP/dz\cdot R_i}{0.32\cdot\rho_g}}\cdot\ln\left(\frac{R_i-r}{26\cdot\dfrac{\mu}{\rho_g}\cdot\sqrt{\dfrac{2\cdot\rho_g}{-dP/dz\cdot R_i}}}\right) \tag{19}$$

where the total pressure gradient and fanning friction factor are approximated by using analytical/empirical equations proved from the Moody friction (Incropera and Dewitt, 2002):

$$-\frac{dP}{dz}\approx\frac{\Delta P}{L}$$

$$\Delta P=-\frac{f\cdot\rho_g\cdot v_{av}^2 L}{4\cdot R_i} \tag{20}$$

$$f=\frac{0.184}{\mathrm{Re}^{0.2}},\ \mathrm{Re}\ \geq\ 20{,}000$$

The average velocity is calculated by

$$v_{av} = \frac{2}{R_i^2}\int_0^{R_i} r v_z(r) dr \tag{21}$$

- The dynamics of tube and wall furnace temperature:

$$\frac{dT_t}{dt} = \frac{1}{\rho_t c_{p,t}} k_t \frac{\partial^2 T_t}{\partial z^2} + \frac{1}{\rho_t c_{p,t} V_{th,t}}\left[A_w F \sigma (T_w^4 - T_t^4) - A_i F \sigma (T_t^4 - T_g^4) - \frac{2\pi L}{\frac{\ln(R_o / R_i)}{k_t} + \frac{1}{R_o h_f}} (T_w - T_t)\right]$$

$$\frac{dT_w}{dt} = \frac{\dot{m}_{fuel} \Delta H_{comb} - \sigma F A_w (T_w^4 - T_t^4)}{(m_w c_{p_w})} \tag{22}$$

with the boundary and initial conditions:

$$B.C. \begin{cases} T_t(0,t) = T_{t,0} \\ \frac{\partial T_t}{\partial z}(L,t) = 0 \end{cases}$$

$$I.C. \begin{cases} T_t(z,0) = T_{t,0} \\ T_w(z,0) = T_{w,0} \end{cases}$$

All process parameters defined in the notation section are given in Table 1.

Table 1 Parameter values for EDC cracking furnace

Symbol	Quantity	Value
A_w	Area of the furnace wall	218 m^2
C_{pg}	Average heat capacity of cracked gases	8.5059 m^3
C_{pw}	Heat capacity of the furnace wall	1000 L/kg K
D_i	Internal tube diameter	0.19 m
E_a	Activation energy	1.15×10^5 J/mol

Table 1 (continue)

Symbol	Quantity	Value
F	Shape factor	1
ΔH_{EDC}	Heat of reaction	-7.1×10^{4} J/mol
ΔH_{comb}	Heat of combustion	4.25×10^{7} J/mol
k_0	Kinetic constant	1.15×10^{7}
k_g	Thermal conductivity of gases in the tube	2.655×10^{-2} W/m K
k_t	Thermal conductivity of the tube	20.5 W/m K
L	Tube length	300 m
m_t	Tube weight	7.783×10^{3} kg
m_w	Mass of the furnace wall	4.191×10^{5} kg
$\dot{m}_f$	Mass flow rate of the fuel	0-0.6 kg/s
M_{EDC}	EDC molecular weight	98.96 g/mol
M_{coke}	Coke molecular weight	12 g/mol
Pe	Thermal Peclet number	8.57×10^{5} –2.00×10^{6}
Pr	Prandl number	0.72
R	Gas constant	8.314 J/mol K
R_i	Internal tube radius	0.095 m
R_o	External tube radius	0.1 m
Re	Reynolds number	1.19×10^{6} –2.78×10^{6}
V_t	Pipe volume	8.5059 m^3
ρ_g	Cracked gas density	35.43 kg/m^3
ρ_t	Tube density	8470 kg/m^3
ρ_c	Coke density	2162.5 kg/m^3
σ	Stefan-Boltzmann constant	5.67×10^{-8} W/m^2 K
μ	Viscosity of cracked gases	1.695×10^{-5} kg/m s
v	Feed velocity	5 m/s

* The values of density and heat capacity of mixed gas are averaged based on 55% EDC conversion. The actual chemical path that EDC takes to form VCM is considered by ignoring the side reactions of the process.

Source: Kitabatake and Onouch (1962); Office of air quality planning and standards (1984); Perry and Green (1997); Shahrokhi and Nejati (2002); Kaggerud (2007); Occidental Petroleum Corporation (2008)

With the importance of distributed radial direction, the velocity model in Equation (19) is implemented in the EDC cracking model in order to formulate the flow pattern or velocity profile for the gases inside the tube. The velocity profile at the average velocity = 3-7 m/s is shown in Figure 8, and the velocity profile in Figure 8 will be compared in Figure 9 at the same based location to indicate the difference in velocity profiles when the average velocity is changed.

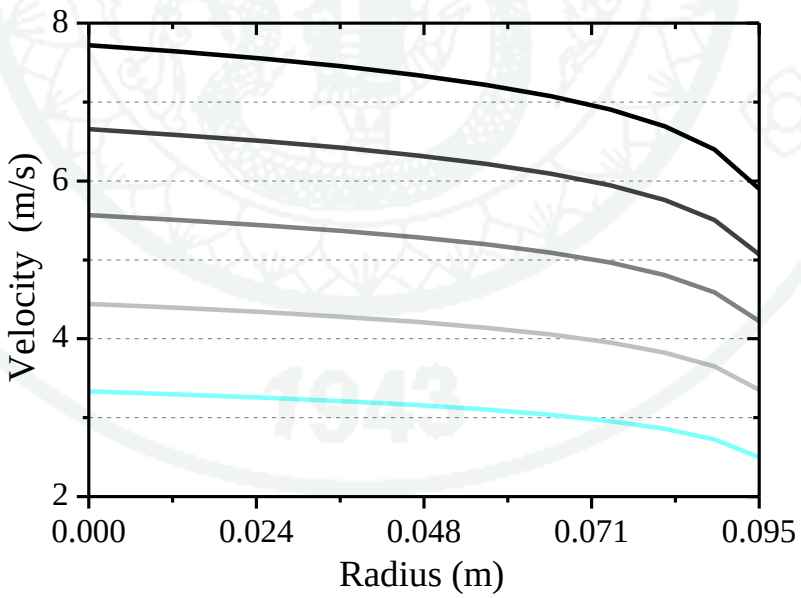

Figure 8 The velocity changing with *r*-direction for v_{av} = 3, 4, 5, 6, and 7 m/s

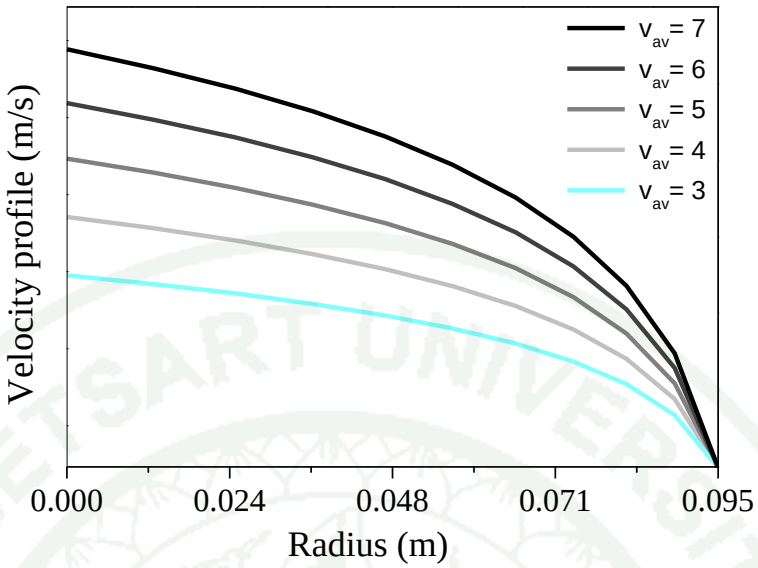

Figure 9 The velocity profile comparison of gas flow under the feed operation

2. The controller performance with the servo and regulatory tests

The velocity with plug-flow pattern is primarily assumed in many literatures for a control of the tubular reactor, but this assumption is proper for a high-viscosity fluid.

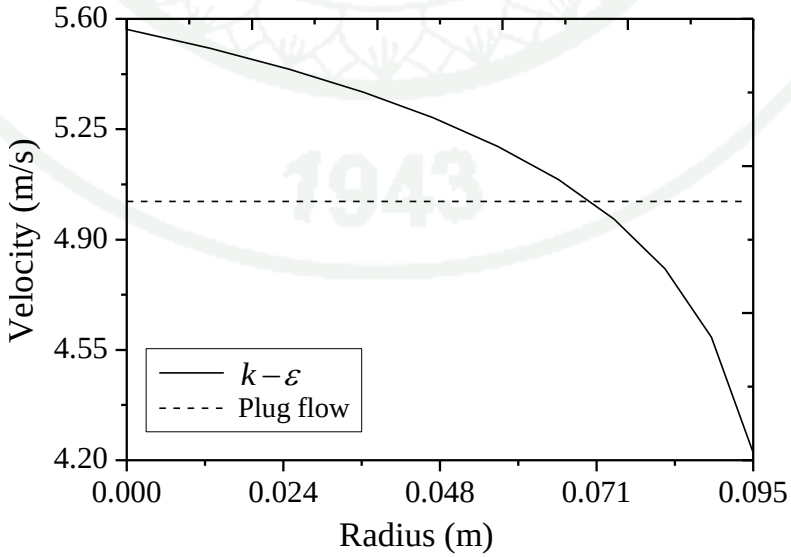

Figure 10 The flow pattern of cracked gas inside the tube

To achieve a realistic prediction, the $k-\varepsilon$ turbulence model is applied with the developed 2D model. For example, the velocity profile based on average velocity = 5 m/s is shown in Figure 10.

The objective is to control the outlet gas temperature (T_g) by manipulating the fuel gas flow ($u = \dot{m}_f$). The control proposed system take steps in the development as follow in Figures 3-6 to find a suitable structure for controlling gas temperature of EDC cracking furnace. The details for each control structure are demonstrated next.

2.1 Initiation of the control system design

At first, the control system design should be developed as Figure 3, but after the controller equation is formulated, it is found that such equation is very long and complex; the controller development and controller equation are shown in Equations (B.1) and (B.2). Therefore, to solve that problem, the I/O controller in Figure 3 is divided into two parts: the setpoint tracking calculator and I/O controller, which is demonstrated in Figure 4. The method used to separate the I/O controller in Figure 3 is indicated in the second step in Figure 2.

2.2 The control system design with the partition controller structure

After the partition controller structure is applied, the controller is divided to be the setpoint tracking calculator and I/O controller. For this partition, it results in the interaction between the two controllers. After the setpoint tracking calculator receives the input (v_T), the output from this part will be the input to the next unit, I/O controller, and the I/O controller will give the manipulated input (u) to the process. The simulation results from the proposed control structure in Figure 4 will be discussed below.

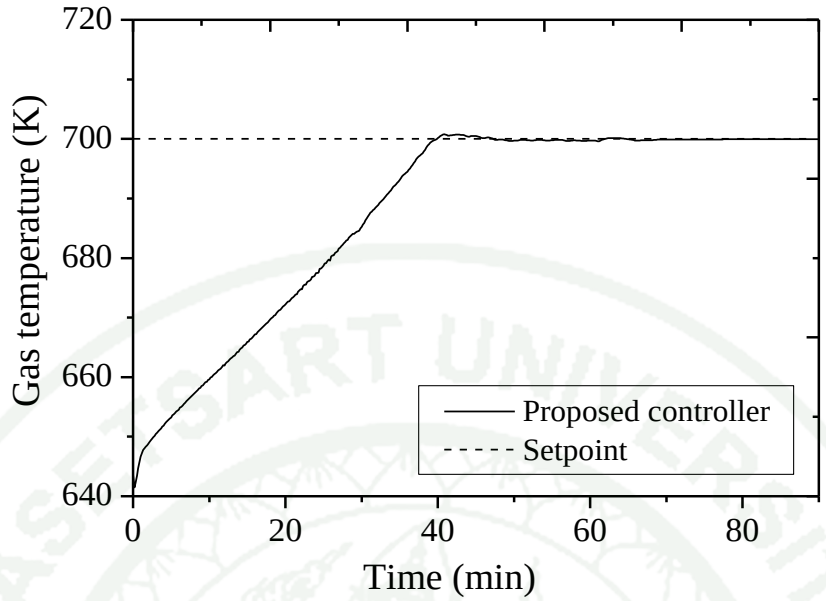

Figure 11 The closed-loop response of the gas temperature at the center exit tube

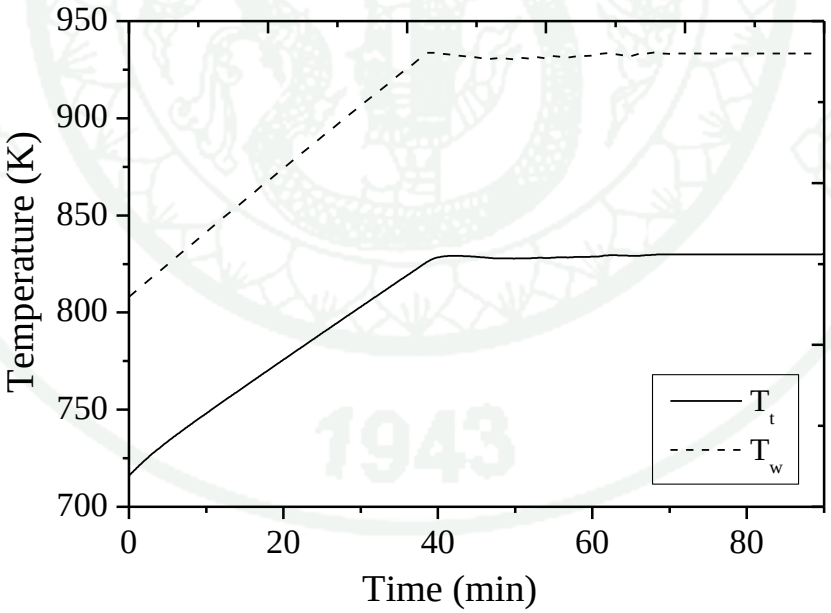

Figure 12 The closed-loop responses of the tube temperature at the exit and wall temperature

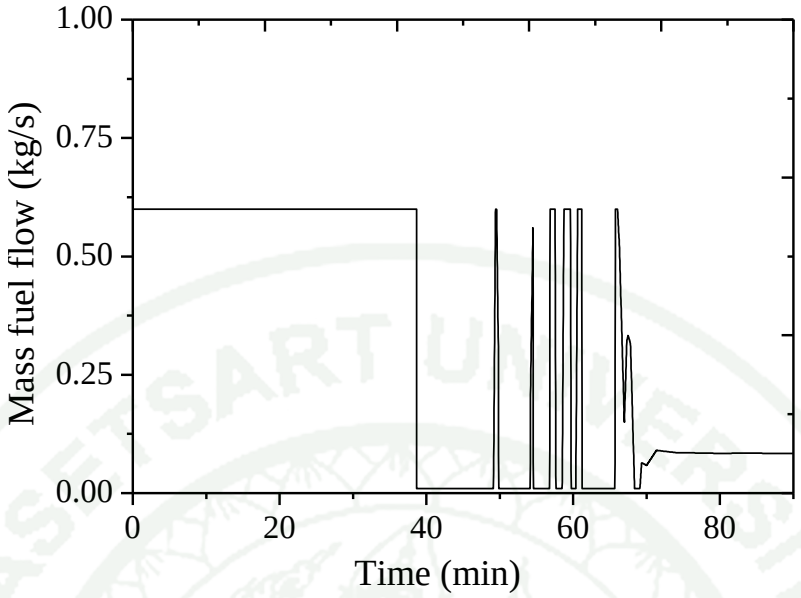

Figure 13 The control action of the manipulated input

For the servo test, the gas temperature at exit tube is controlled at the desired setpoint y_{sp} = 700 K. The initial conditions of the dynamics are C_{EDC} *(r,0,t)* = 359.83 mol/l, T_g *(r,0,t)* = 644 K, T_t *(0,t)* = 716 K, and T_w = 808 K. In this case, the velocity of gas is equal to 5 m/s and its velocity profile is shown in Figure 10. The tuning parameters of the proposed control system are β_1 = 8, β_2 = 8 and λ = 0.001. The closed-loop responses of the cracking furnace are illustrated in Figures 11-13.

The results show that the controller successfully forces the gas temperature at the desired setpoint. The changes of gas, tube and wall temperature at the initial period have a linear trend due to the influence from the constant of fuel gas rate at the upper limit. Then, the controller will adjust the fuel gas flow with a little fuzzy to put the gas temperature at the desired setpoint. Such the fuzzy mainly occurs from a small value of β_2. If β_2 is increased, that problem should be fixed. Nevertheless, an important problem is the implementing the first-order error dynamics in COMSOL. For example, the controller is tested with the servo test. After the gas temperature is forced to the first desired setpoint at 700K, this integrator needs to set the initial value to zero before approaching the next setpoint. In COMSOL, setting the initial value of the integrator cannot be done for a simulation, and if the simulation is separated, it may cause

uncontinuity of the data. Moreover, it about the ability in compensating the process model mismatch between the controlled output and setpoint. In order to receive a better compensation, a new integrator in Equation (18) is developed and applied to the controllers in Figure 5.

2.3 The partition controller structure with the new integrator

According to Figure 5, the tracking compensator is applied with the partition controller system to eliminate the offset of the controlled output (T_g) and the desired setpoint. With the structure in Figure 5, this compensator must compensate both the error which occurs in the setpoint tracking calculator and the I/O controller. In this research, the performance of the controller is measured with the servo and regulatory tests.

2.3.1 Servo test

The initial conditions of the case study are shown as follows. The gas temperature at exit tube is controlled at the desired setpoint y_{sp} = 700 K. The initial conditions of the dynamics are $C_{EDC}(r,0,t)$ = 359.83 mol/l, $T_g(r,0,t)$ = 644 K, $T_t(0,t)$ = 716 K, and T_w = 808 K. The tuning parameters of the proposed control system are β_1 = 9, β_2 = 7 and ε = 1500. From the previous part, if β_1 and β_2 are tuned with the same value, the response of the manipulated input ($\dot{m}_f$) will be aggressive as shown in Figure 13. In order to avoid such behavior, the value of β_2 will be large to reduce the fast moving of the controller, while β_1 is a little bit bigger; if the value of β_1 is increased too much, the controller will not drive the controlled output at the desired setpoints. In this system, the tuning parameter of the setpoint tracking calculator is around ten. Then, suitable values of β_2 and ε will be determined by the change of the manipulated input ($\dot{m}_f$). Figures 14-16 illustrate the responses of the controlled output (T_g) and the other state variables (T_t , T_w and C_{edc}).

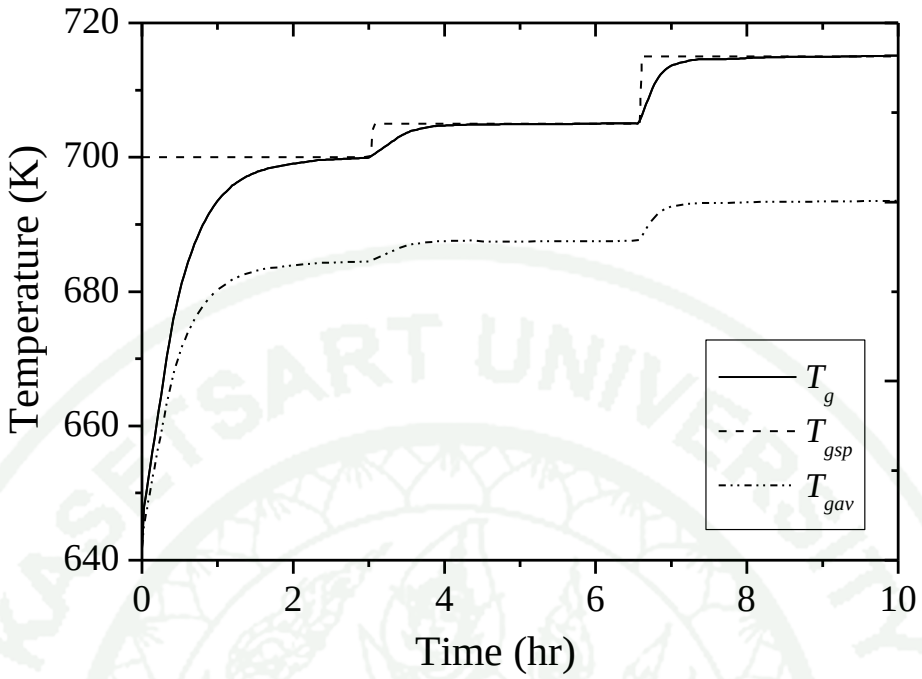

Figure 14 Closed-loop response of the gas temperature at the center of the exit and the average gas temperature along the tube under the servo test

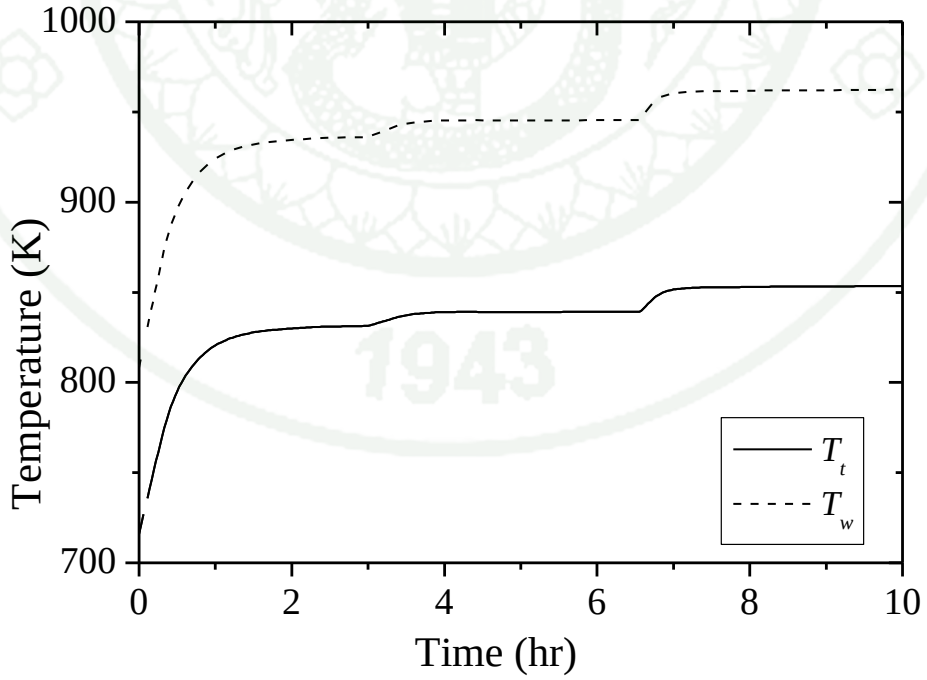

Figure 15 Closed-loop responses of the outlet tube temperature and the furnace wall temperature under the servo test

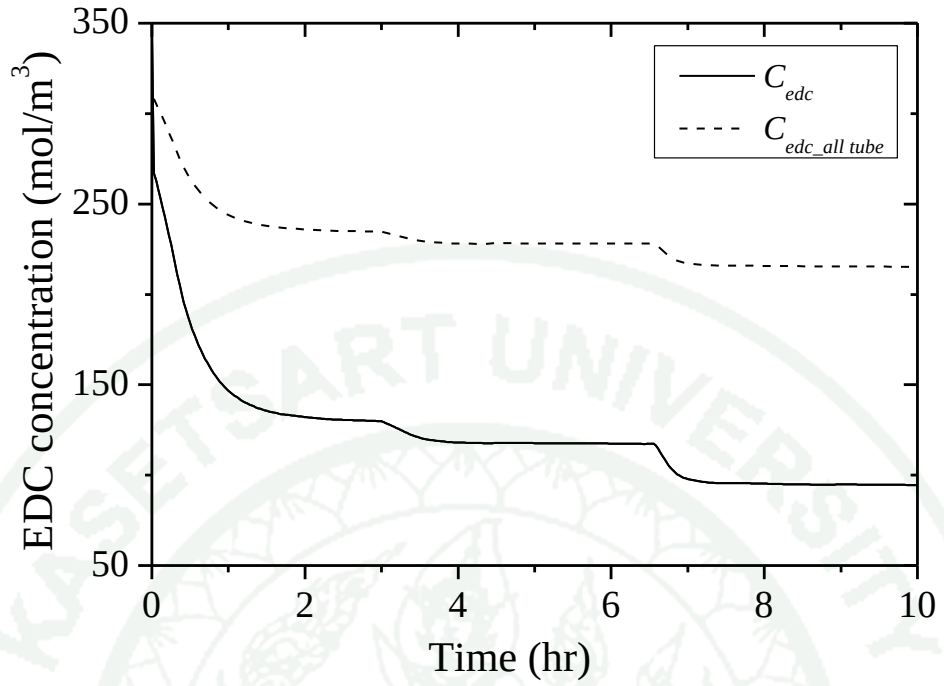

Figure 16 Closed-loop responses of the EDC concentration at the center of the exit and the average EDC concentration along the tube under the servo test

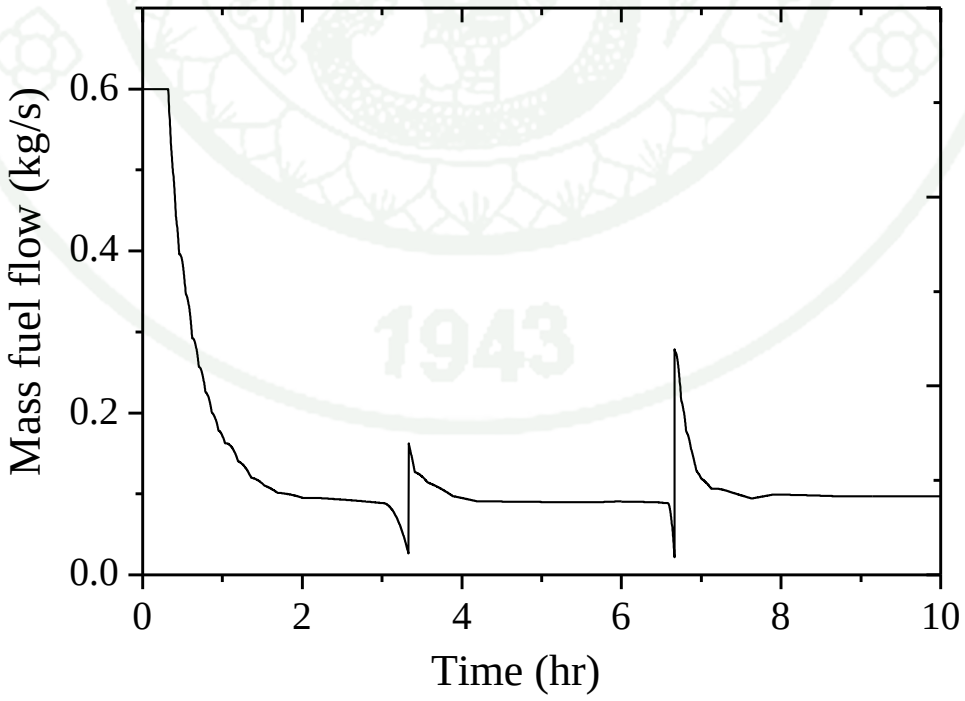

Figure 17 The control action of the manipulated input under the servo test

The results show that the controller can drive the controlled output (T_g) at the desired setpoint asymptotically. The changes of the tube temperature, furnace wall temperature and EDC concentration are reasonable with the gas temperature change. In Figure 14, the setpoint of gas temperature is increasingly moved for 5 and 10 K, it leads to an increase on mass fuel flow.

2.3.2 Regulatory test

In this work, the proposed control system is tested with the measured disturbance; the variations of EDC feed flow rate are changed from 18 ton/hr to 14.5 ton/hr ($v_{av} = 5 \rightarrow 4\ m/s$) and from 18 ton/hr to 21.7 ton/hr ($v_{av} = 5 \rightarrow 6\ m/s$). The simulation results of each case are illustrated as follow.

2.3.2.1 Measured disturbance from the reduction of EDC feed flow

The initial conditions and the tuning parameters of this test are the same as 2.3.1, but after the controlled output (T_g) reaches the desired setpoint (T_{gsp} = 700), at t = 3.33 h the EDC feed rate is changed from 18 to 14.5 ton/h. Figures 18-20 illustrate the responses of the controlled output (T_g) and the other state variables (T_t , T_w and C_{edc}) when the EDC feed flow is decreased.

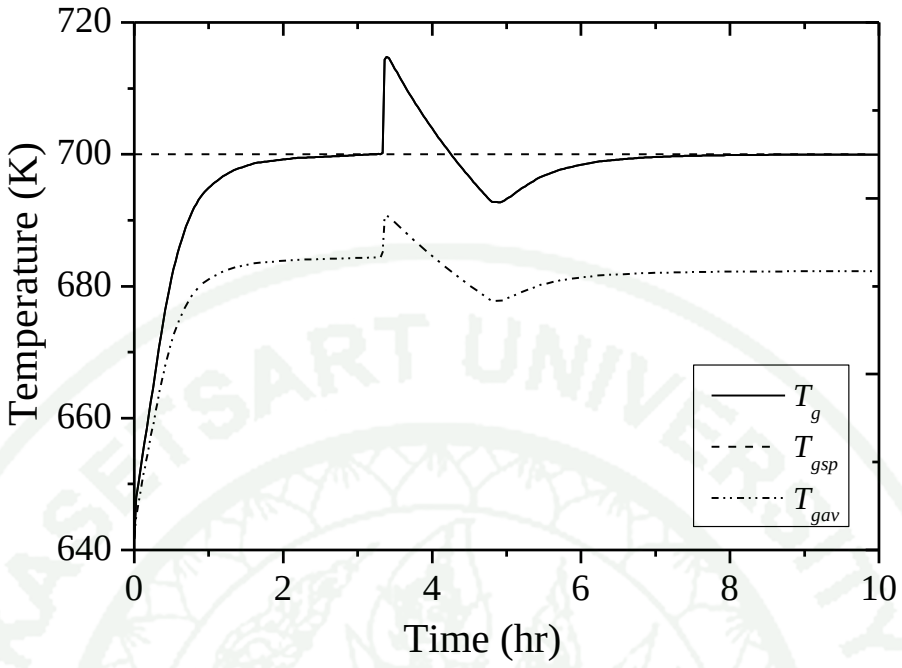

Figure 18 Closed-loop response of the gas temperature at the center of the exit and the average of the gas temperature along the tube with the change of EDC feed flow rate from 18 to 14.5 ton/hr

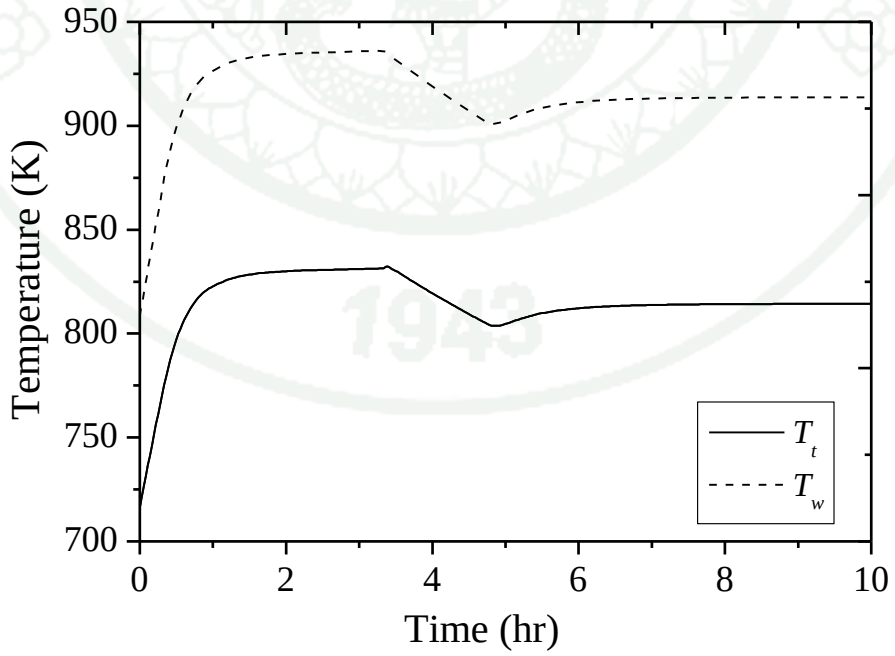

Figure 19 Closed-loop responses of the outlet tube temperature and the furnace wall temperature with the change of EDC feed flow rate from 18 to 14.5 ton/hr

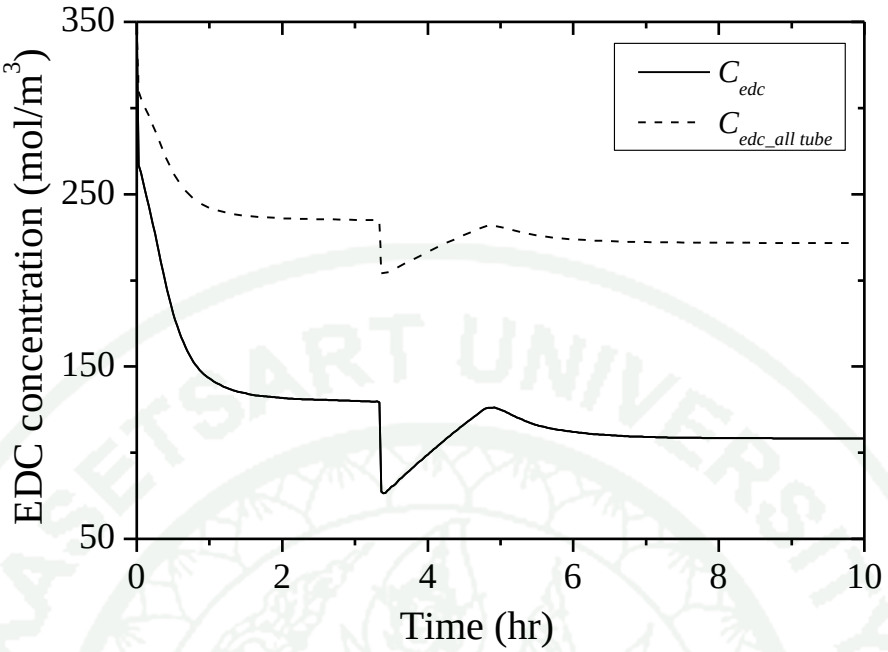

Figure 20 Closed-loop responses of the EDC concentration at the center of the exit and the average concentration of EDC along the tube with the change of EDC feed flow rate from 18 to 14.5 ton/hr

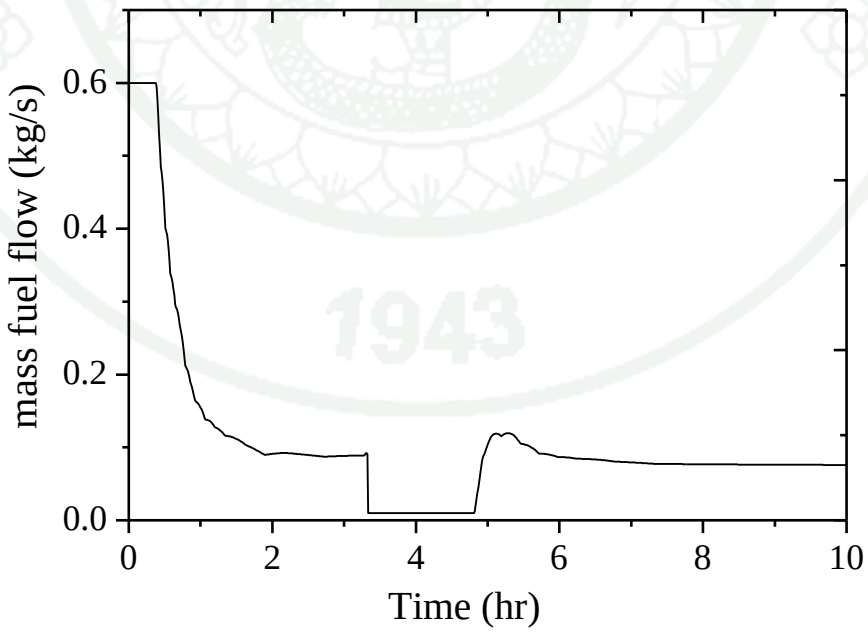

Figure 21 The control action of the manipulated input under the regulatory test in case of the reduction in EDC feed flow rate

The results show that the controller can reject the disturbance from the decrease in the feed flow of EDC. The controlled output (T_g) is forced to the desired setpoint smoothly. The behaviors of the tube temperature and furnace wall temperature are the same trend with the change of gas temperature but vice versa in EDC concentration behavior. According to Figure 34, when the gas temperature is more increased than the desired setpoint, the manipulated input will decrease simultaneously to move the controlled output to the desired setpoint.

2.3.2.2 Measured disturbance from the increase on EDC feed flow

The initial conditions and the tuning parameters of this test are also the same as 2.3.1, but after the controlled output (T_g) reaches the desired setpoint (T_{gsp} = 700), the EDC feed rate will be increased from 18 to 21.7 ton/h at t = 3.33 h. Figures 36-38 illustrate the responses of the controlled output (T_g) and the other state variables (T_t , T_w and C_{edc}) when the EDC feed flow is increased.

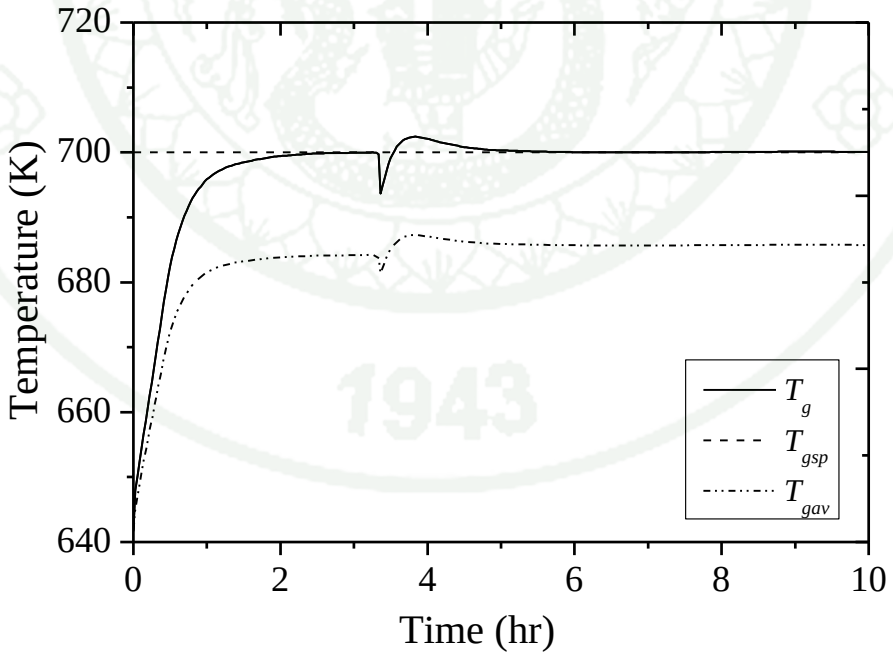

Figure 22 Closed-loop response of the gas temperature at the center of the exit and the average of the gas temperature along the tube with the change of EDC feed flow rate from 18 to 21.7 ton/hr

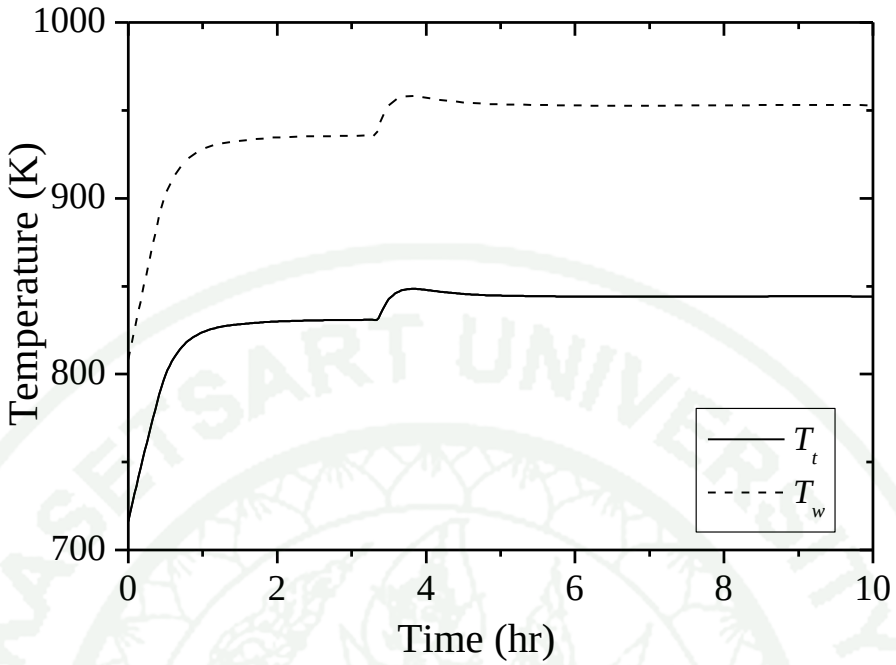

Figure 23 Closed-loop responses of the outlet tube temperature and the furnace wall temperature with the change of EDC feed flow rate from 18 to 21.7 ton/hr

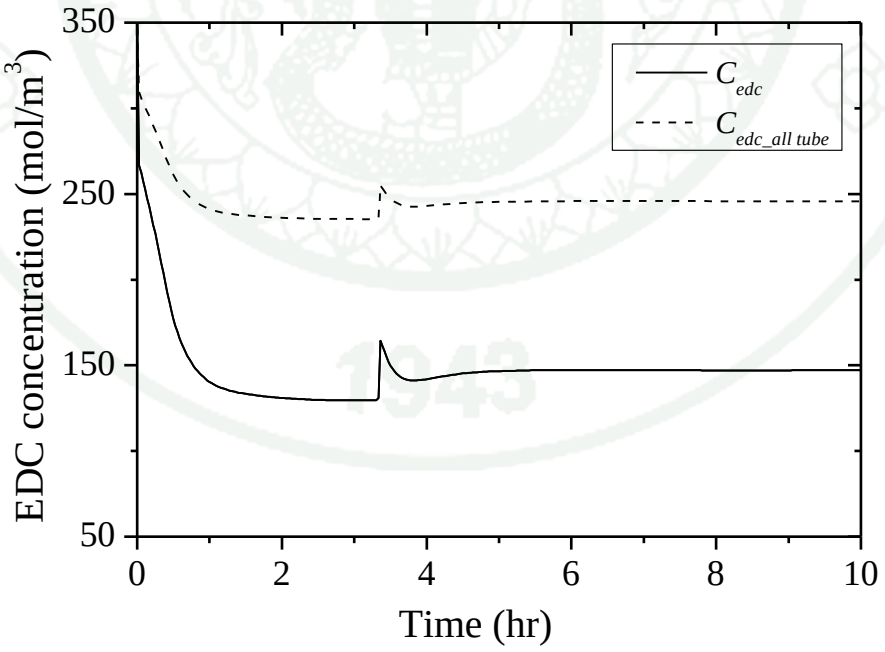

Figure 24 Closed-loop responses of the EDC concentration at the center of the exit and the average concentration of EDC along the tube with the change of EDC feed flow rate from 18 to 21.7 ton/hr

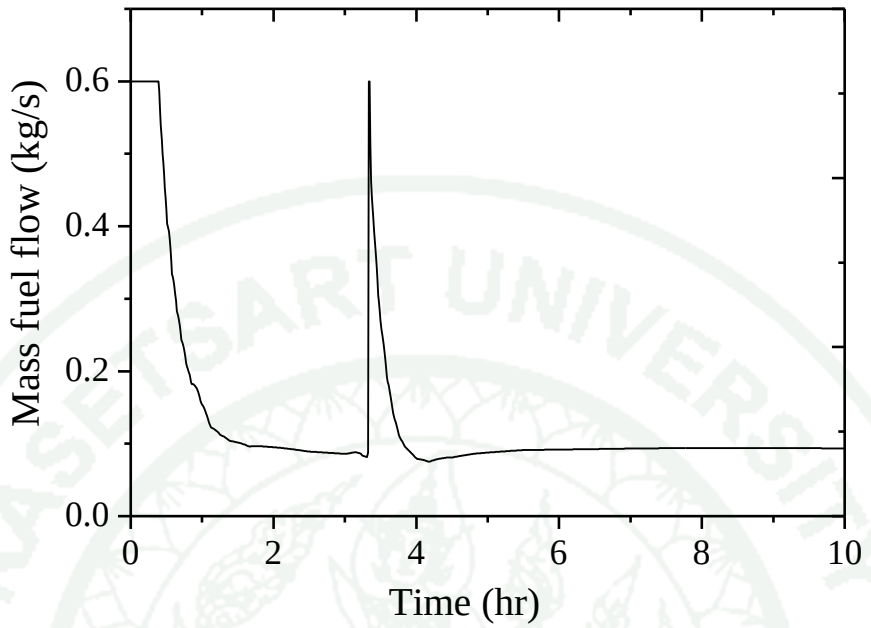

Figure 25 The control action of the manipulated input under the regulatory test in case of the increase on EDC feed flow rate

The proposed control system can reject the disturbance from the increase on the feed flow of EDC as in the case of decrease in EDC feed flow. The changes of tube temperature, furnace wall temperature and EDC concentration behave the opposite way from the reduction of EDC feed flow case. However, the interesting point in Figure 31 compared to Figure 36 is the behaviors of gas temperature; it implies that it is easier for control to increase the temperature rather than decrease.

2.4 The cascade structure with the new integrator

According to the problems in 2.3, all error is compensated with the outer loop of the integrator, which brings about the question when the cascade loop is implemented. Therefore, the control system design in Figure 6 demonstrates the cascade structure for control loop. The integrator in the structure will compensate the mismatch between the controlled output (T_g) and manipulated input (T_{gsp} and χ) of

the setpoint tracking calculator and the I/O controller. The performance and robustness of the proposed controller are evaluated through servo and regulatory tests.

In Figure 6, there are four tuning parameters for the cascade control loop where β_1 and ε_1 are the tuning parameters of the setpoint tracking calculator and the outer loop compensator,as well as β_2 and ε_2 are the tuning parameters of the I/O controller and inner loop compensator, respectively. The first step for tuning the parameters is to find a suitable coupling between β_2 and ε_2 by giving a constant (χ) which makes $T_g = 700K$; these suitable values of β_2 and depend on the change of slope in manipulated input ($\dot{m}_f$) as shown in Figure 20 at t = 0-3 h. the change of ε_2 is based on the value of β_2; one value of β_2 relates to only a suitable value of ε_2, which is fixed by desired asymptotic crave of the controlled output (T_g) as shown in Figure 17 at t = 0-3 h. After the appropriate β_2 and ε_2 are received, a coupling of β_1 and ε_1 will be found next.

2.4.1 Servo test

For the servo test, the gas temperature at exit tube is controlled at the desired setpoint y_{sp} = 700 K. The initial conditions of the dynamics are C_{EDC} *(r,0,t)* = 359.83 mol/l, T_g *(r,0,t)* = 644 K, T_t *(0,t)* = 716 K, and T_w = 808 K. The tuning parameters of the proposed control system are β_1 = 10, β_2 = 150, ε_1 = 1600 and ε_2 = 400. Then, at time = 3.33 and 6.66 hr, the desired setpoint (y_{sp}) will be changed to 705 and 715 K, respectively. Figures 26-28 illustrate the responses of the controlled output (T_g) and the other state variables (T_t , T_w and C_{edc}).

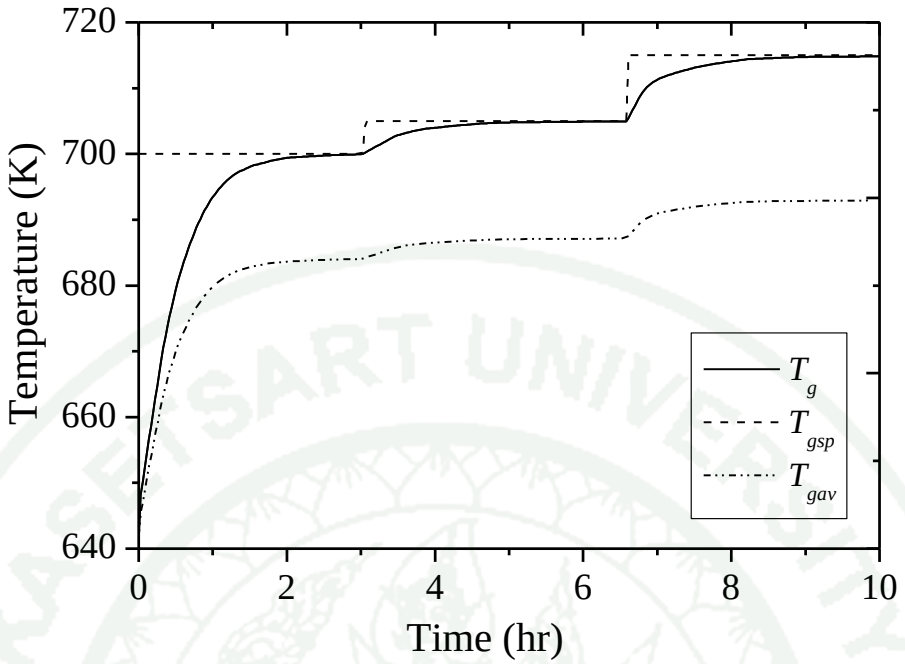

Figure 26 Closed-loop response of the gas temperature at the center of the exit and the average gas temperature along the tube under the servo test

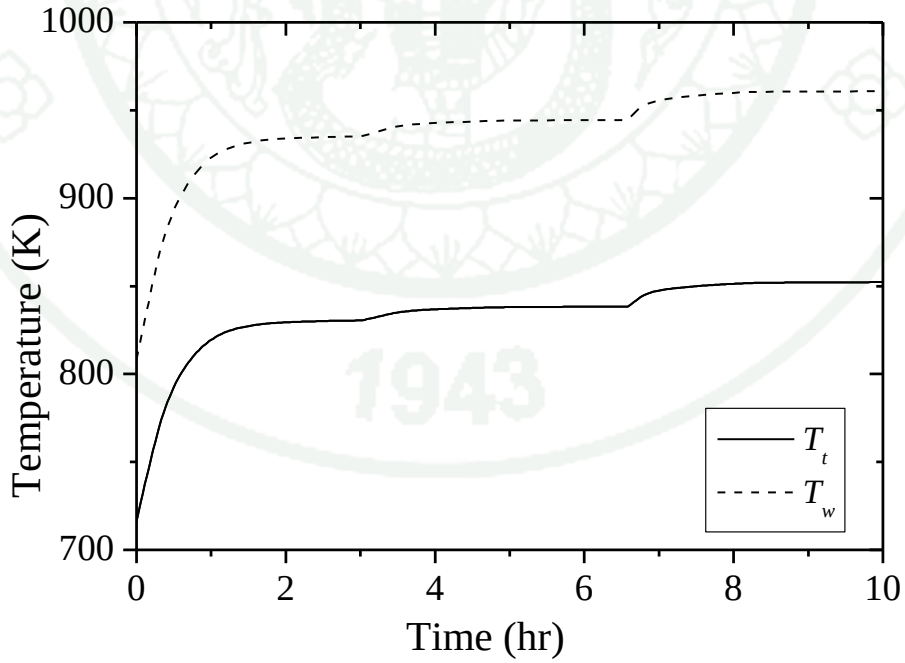

Figure 27 Closed-loop responses of the outlet tube temperature and the furnace wall temperature under the servo test

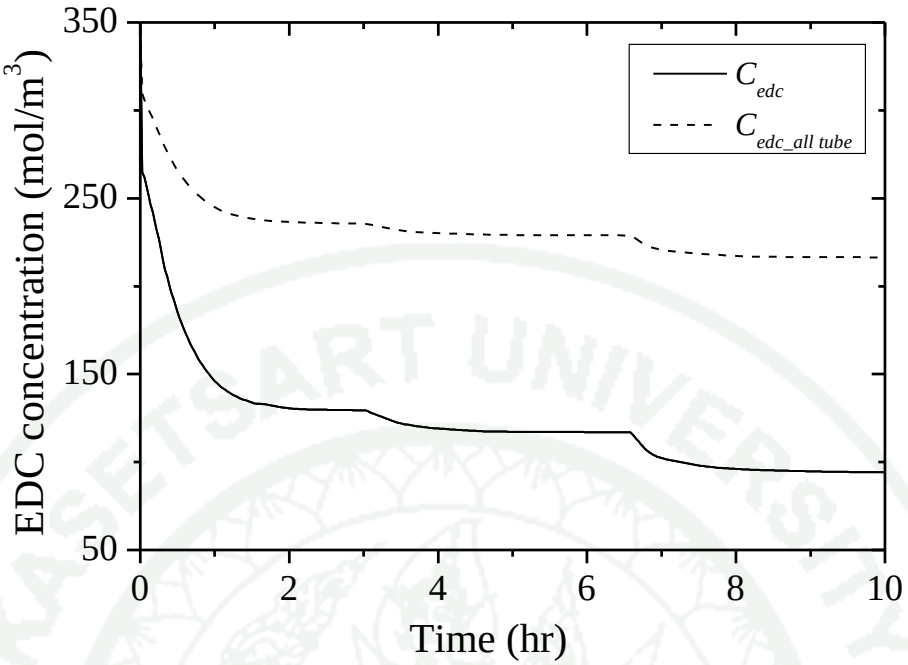

Figure 28 Closed-loop responses of the EDC concentration at the center of the exit and the average EDC concentration along the tube under the servo test

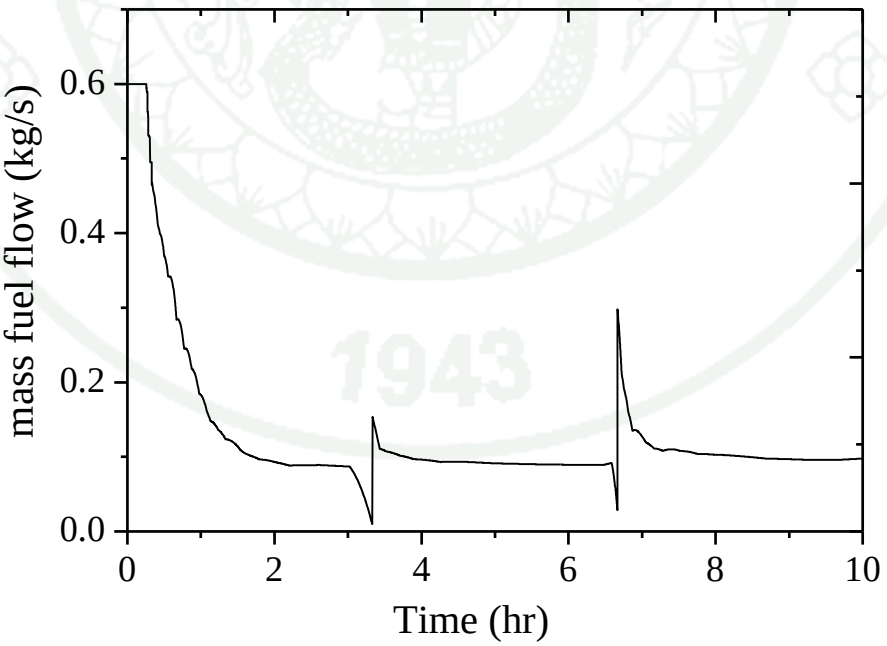

Figure 29 The control action of the manipulated input under the servo test

The results show that the controller can force the controlled output (T_g) at the desired setpoint asymptotically. The behaviors of the tube temperature, furnace wall temperature and EDC concentration are the reasonable trend with the change of gas temperature. According to Figure 29, when the desired setpoint of the gas temperature is increased 5 and 10 K, it leads to an increase on mass fuel flow. Though there some peaks between the step changes, the manipulated input ($\dot{m}_f$) has an excellent response for implementing with the real process. Additionally, the distribution of the gas temperature along r and z directions at T_{gsp} = 700 K and $v_{av} = 5\ m/s$ is shown in Figure 30.

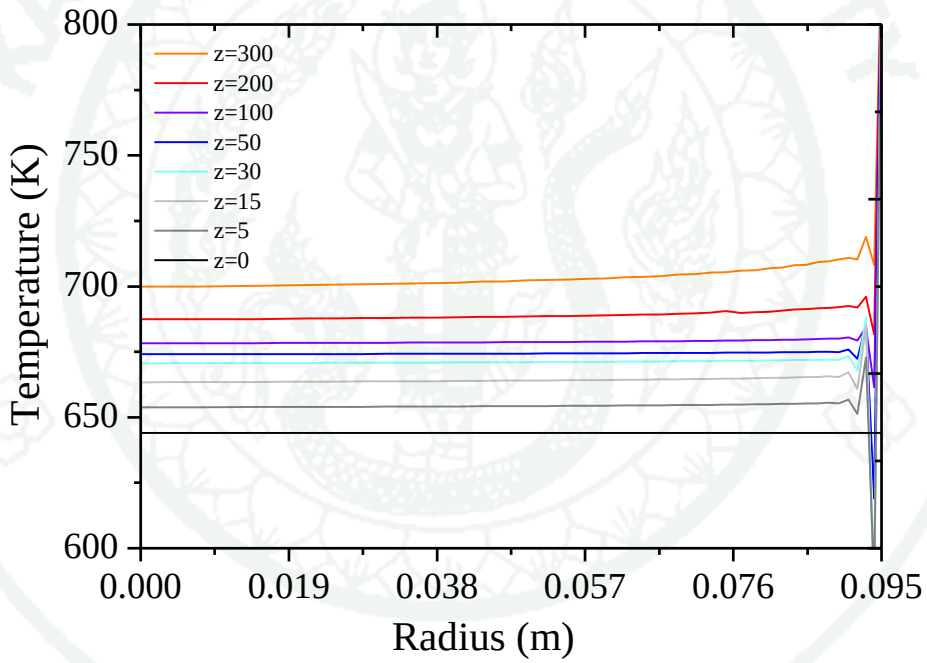

Figure 30 The distribution of gas temperature in r and z-directions at the setpoint $T_g = 700K$ and $v_{av} = 5\ m/s$

2.4.2 Regulatory test

In this work, the proposed control system is tested with the measured disturbance; the variations of EDC feed flow rate are changed from 18 ton/hr to 14.5

ton/hr ($v_{av} = 5 \rightarrow 4\ m/s$) and from 18 ton/hr to 21.7 ton/hr (v_{av}=$5 \rightarrow 6\ m/s$). The simulation results of each case are illustrated as follow.

2.4.2.1 Measured disturbance from the reduction of EDC feed flow

The initial conditions and the tuning parameters of this test are the same as 2.4.1, but after the controlled output (T_g) reaches the desired setpoint (T_{gsp} = 700), at t = 3.33 hr the EDC feed rate is changed from 18 to 14.5 ton/hr. Figures 31-33 illustrate the responses of the controlled output (T_g) and the other state variables (T_t , T_w and C_{edc}) when the EDC feed flow is decreased.

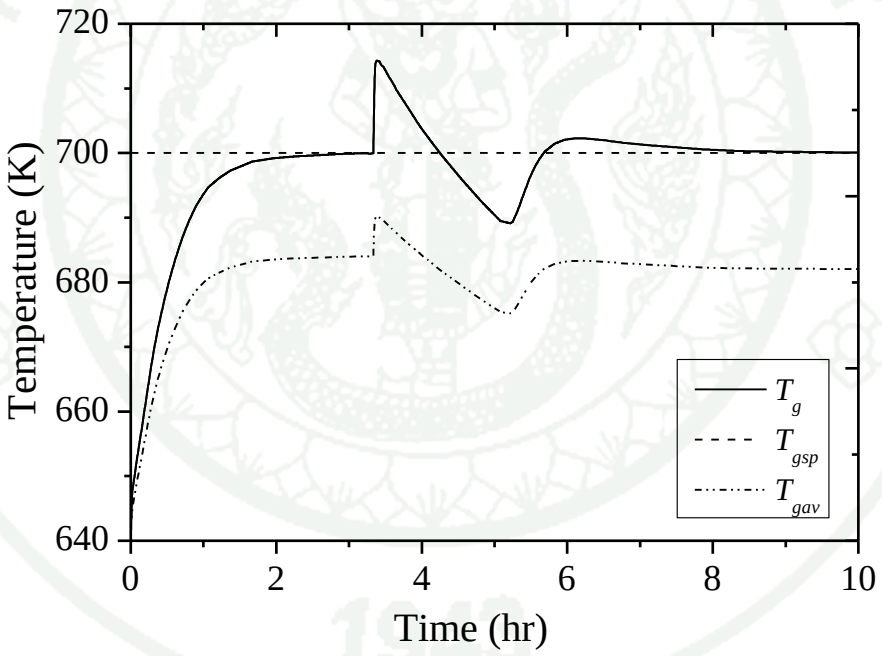

Figure 31 Closed-loop response of the gas temperature at the center of the exit and the average of the gas temperature along the tube with the change of EDC feed flow rate from 18 to 14.5 ton/hr

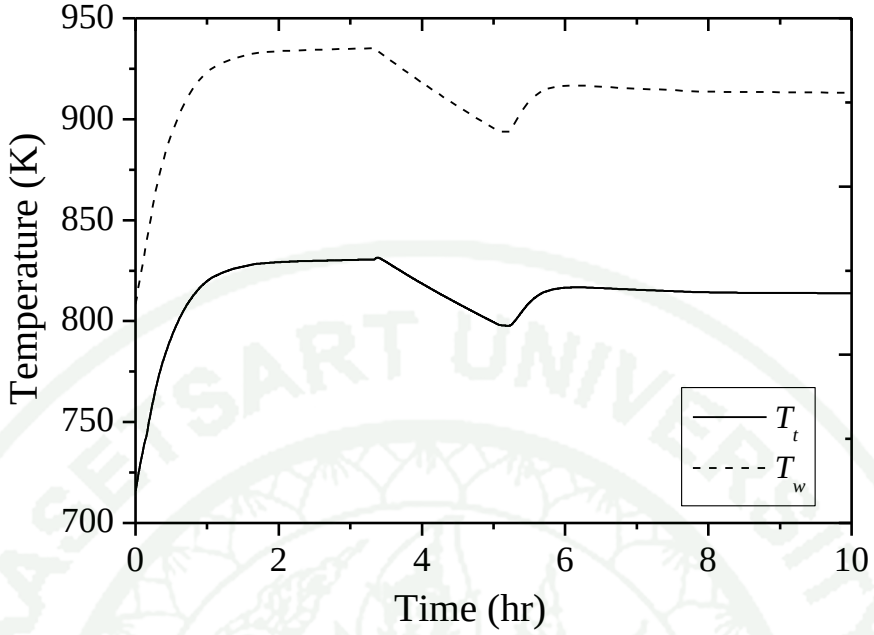

Figure 32 Closed-loop responses of the outlet tube temperature and the furnace wall temperature with the change of EDC feed flow rate from 18 to 14.5 ton/hr

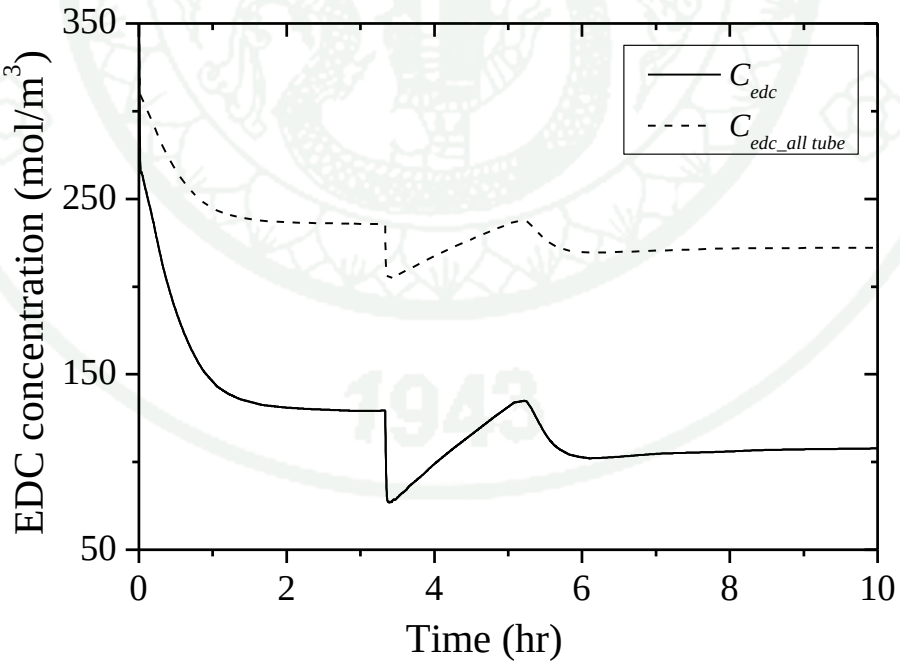

Figure 33 Closed-loop responses of the EDC concentration at the center of the exit and the average concentration of EDC along the tube with the change of EDC feed flow rate from 18 to 14.5 ton/hr

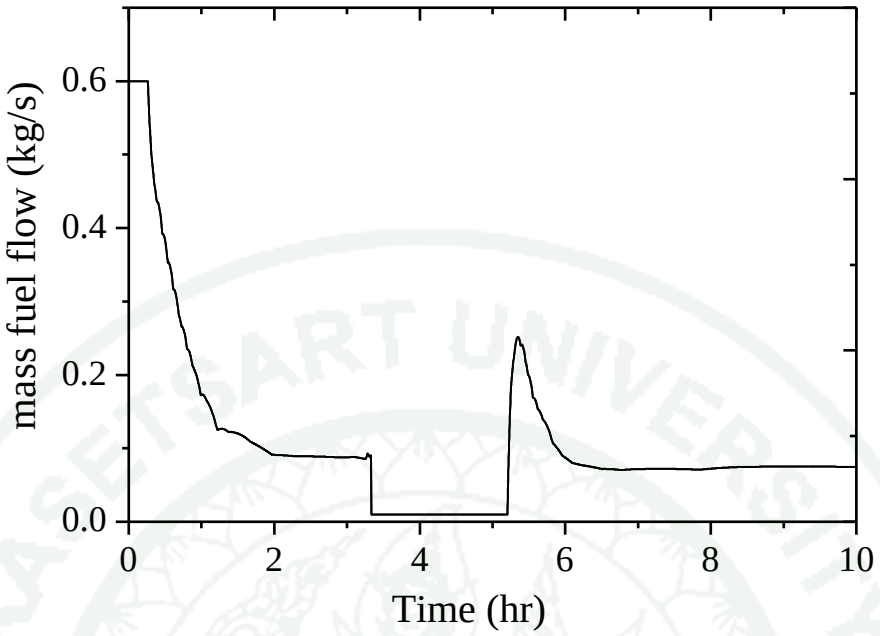

Figure 34 The control action of the manipulated input under the regulatory test in case of the reduction in EDC feed flow rate

The results show that the controller can reject the disturbance from the decrease in the feed flow of EDC. The controlled output (T_g) is forced to the old desired setpoint smoothly. The behaviors of the tube temperature and furnace wall temperature are the same trend with the change of gas temperature but vice versa in EDC concentration behavior. According to Figure 34, when the gas temperature is more increased than the desired setpoint, the manipulated input will decrease simultaneously to move the controlled output to the desired setpoint. In addition, the distribution of the gas temperature along r and z directions at T_{gsp} = 700 K for disturbance test ($v_{av} = 4\ m/s$) is shown in Figure 35.

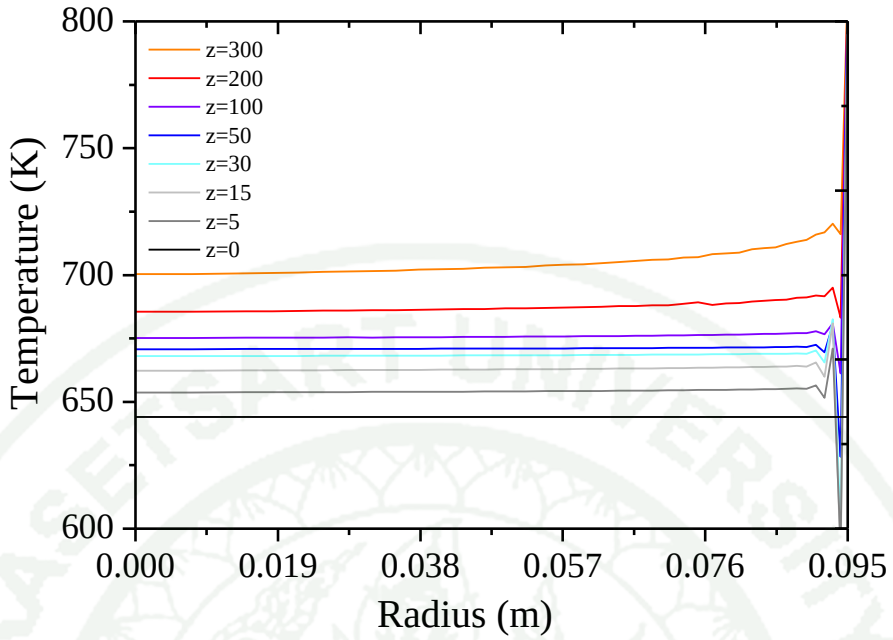

Figure 35 The distribution of gas temperature in *r* and *z*-directions at the setpoint $T_g = 700K$ and $v_{av} = 4\ m/s$

2.4.2.2 Measured disturbance from the increase on EDC feed flow

The initial conditions and the tuning parameters of this test are also the same as 2.4.1, but after the controlled output (T_g) reaches the desired setpoint (T_{gsp} = 700), the EDC feed rate will be increased from 18 to 21.7 ton/hr at t = 3.33 hr. Figures 36-38 illustrate the responses of the controlled output (T_g) and the other state variables (T_t , T_w and C_{edc}) when the EDC feed flow is increased.

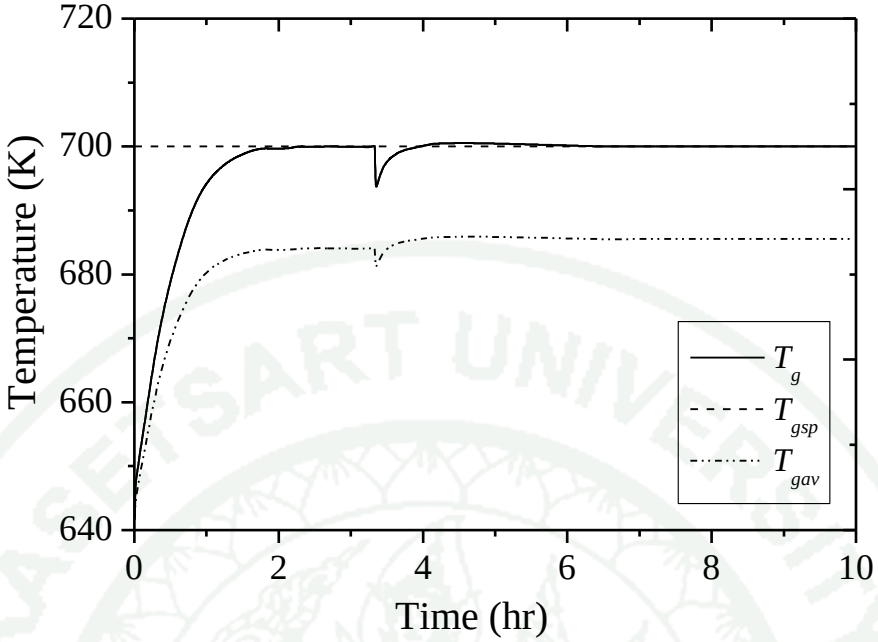

Figure 36 Closed-loop response of the gas temperature at the center of the exit and the average of the gas temperature along the tube with the change of EDC feed flow rate from 18 to 21.7 ton/hr

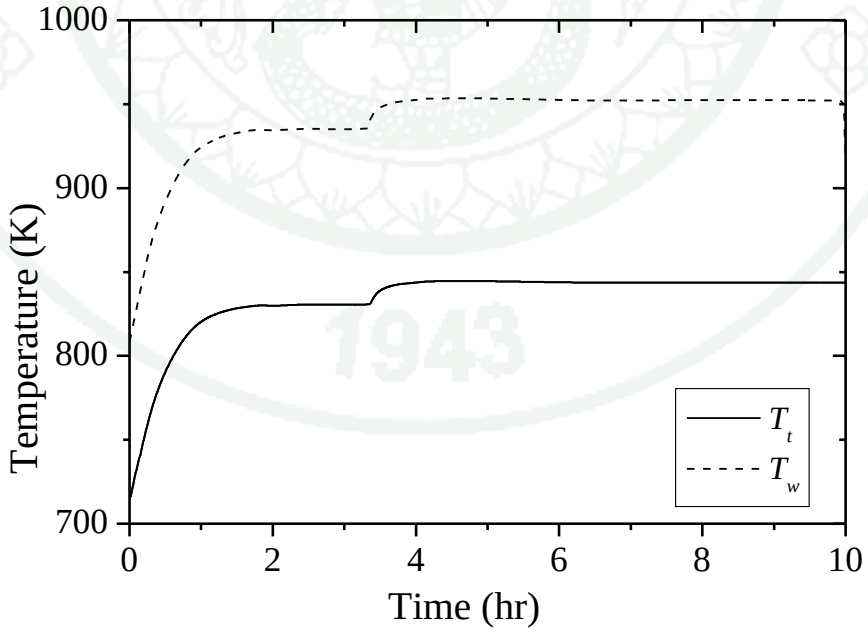

Figure 37 Closed-loop responses of the outlet tube temperature and the furnace wall temperature with the change of EDC feed flow rate from 18 to 21.7 ton/hr

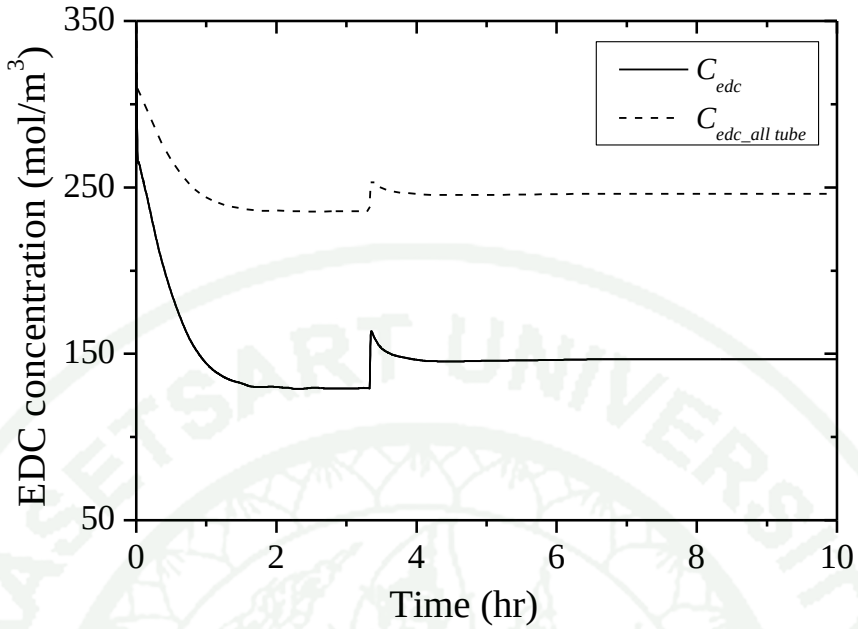

Figure 38 Closed-loop responses of the EDC concentration at the center of the exit and the average concentration of EDC along the tube with the change of EDC feed flow rate from 18 to 21.7 ton/hr

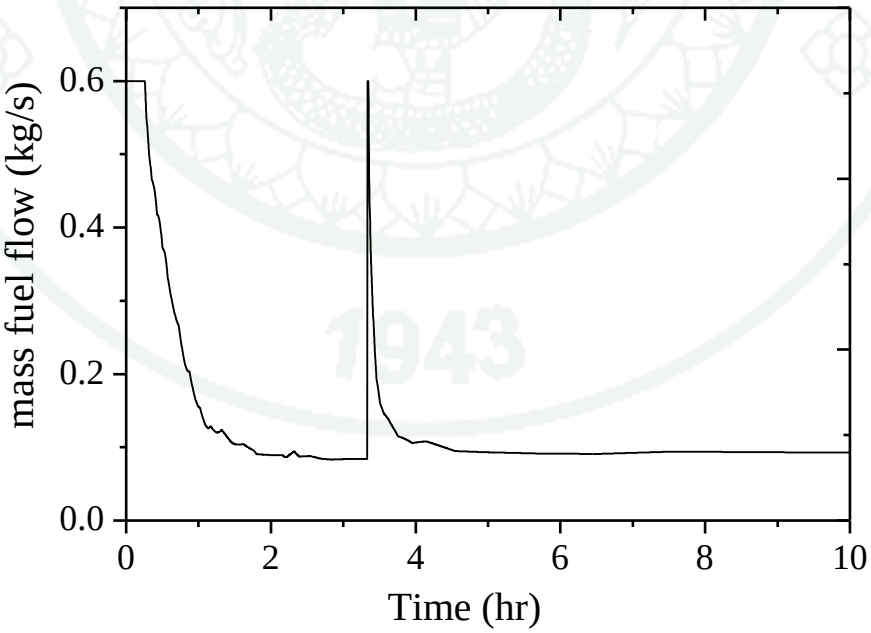

Figure 39 The control action of the manipulated input under the regulatory test in case of the increase on EDC feed flow rate

The proposed control system can reject the disturbance from the increase on the feed flow of EDC as in the case of decrease in EDC feed flow. The changes of tube temperature, furnace wall temperature and EDC concentration behave the opposite way from the reduction of EDC feed flow case. However, the interesting point in Figure 31 compared to Figure 36 is the behaviors of gas temperature; it implies that it is easier for control to increase the temperature rather than decrease. The distribution of the gas temperature along r and z directions at T_{gsp} = 700 K for $v_{av} = 6\ m/s$ is shown in Figure 32.

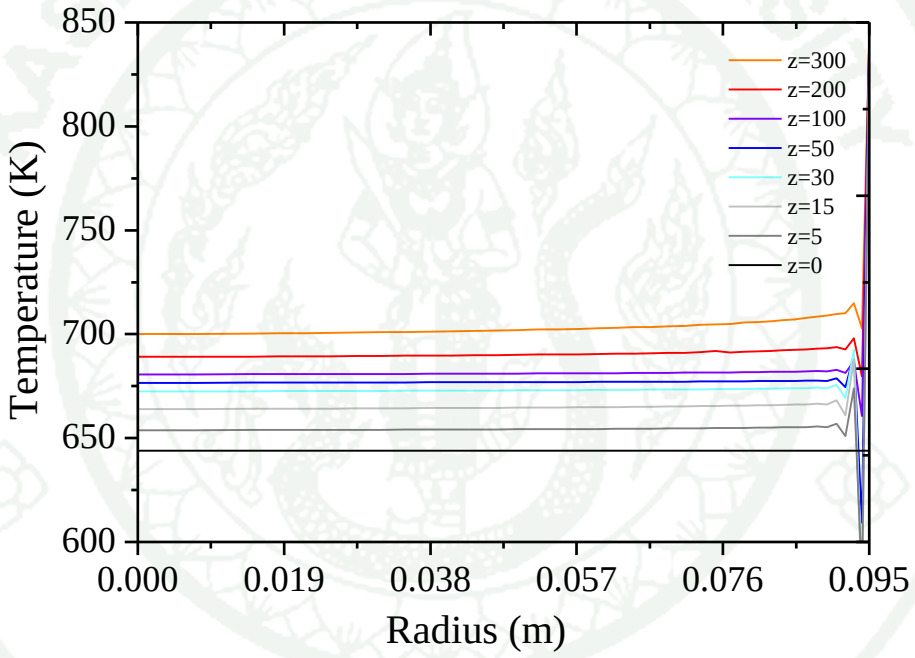

Figure 40 The distribution of gas temperature in r and z-directions at the setpoint $T_g = 700K$ and $v_{av} = 6\ m/s$

According to all of the results, only the partition structure can force the controlled output (T_g) to the desired setpoints with no aggressive behavior of the manipulated input ($\dot{m}_f$). For partition cases in Figures 5 and 6, they are used for a compared case so as to measure the controller performance for control structures composing of an outer loop compensator or a cascade loop compensator. In this work, the tuning parameter of the setpoint tracking calculator and I/O controller of the two cases (β_1 and β_2) are used the same values in order to show the responses in the EDC cracking process. Both results in 2.3 and 2.4 show similar responses for servo and regulatory tests. However, for the controlled structure in 2.3, the responses will be aggressive more than those in 2.4, such as the response in Figure 22 compared to Figure 36 and in Figure 36 compared to Figure 39. For in case 2.3, if β_2 is increased and ε is reduced, the responses will be able to case 2.4. Additionally, in the regulatory test, the process model mismatch from parametric uncertainty of the setpoint tracking calculator and I/O controller should be tested; the responses will be different.

CONCLUSION AND RECOMMENDATION

Conclusion

A new controller structure with I/O linearization technique is developed for the EDC cracking furnace, of which the advantages are a few tuning parameters and decrease on the complexity of the controller equation. With the importance of the distribution in *r*-direction of fluid flow in the tube, the $k-\varepsilon$ turbulent model is applied to the velocity. The controller is formulated with the 2D-PDEs and ODE into the setpoint tracking calculator and I/O feedback controller, and integrated with the tracking compensator dynamics and finite-based, open-loop observer. The setpoint tracking calculator is used to calculate the desired tube temperature to drive the gas temperature to the target. The control system design ensures the offset-free of the closed-loop output responses for the presence of the disturbances and model-process mismatch. The simulation results show that the controller can force the control output at the desired setpoint asymptotically and reject disturbance from the servo and regulatory tests.

Recommendation

In this work, the proposed control system is designed to control the gas temperature. There are many structures developed to find a suitable control structure for controlling the gas temperature which considers the effects of cracking coil and furnace wall. The gas temperature is the control output while the mass fuel flow is the manipulated input. Although I/O linearization technique will be applied directly to control the gas temperature by manipulating the mass fuel flow, which causes the complexity of controller equation, the proposed control system design can solve such a problem. Additionally, the new compensator is formulated to receive a better control performance. The proposed controller can force the gas temperature to the desired setpoint asymptotically. However, there is a problem about the CFD observer which uses a long time for simulation. Therefore, when it has to implement with the real process, the point in this should be developed next.

LITERATURE CITED

Aggelogiannaki, E. and H. Sarimveis. 2009. Robust nonlinear H ∞ control of hyperbolic distributed parameter systems. **Control.Eng. Pract.** 17: 723-732.

Borsa, A. G., A. M. Herring, J. T. McKinnon, R. L. McCormick, S. Yamamoto, Y. Teraoka, and Y. Natori. 1999. Characterization of Coke Formed in Vinyl Chloride Manufacture. **Ind. Eng. Chem. Res.** 38(11): 4259-4267.

Borsa, A. G., A.M. Herring, J.T. McKinnon, R. L. McCormick and G.H. Lo. 2001. Coke and byproduct formation during 1, 2-dichloroethane pyrolysis in a laboratory tubular reactor. **Ind. Eng. Chem. Res.** 40: 2428-2436.

Han, Y.L., Xiao, R., Zhang, M.Y. 2007. Combustion and Pyrolysis Reactions in a Naphtha Cracking Furnace. **Chem. Eng. Technol.** 30: 112-120.

Hoo,K.A. and D.Zheng. 2001. Low-order control-relevant models for a class of distributed parameter systems.**Chem. Eng. Sci.** 56: 6683-6710.

Incavo, J. A. 1996. A detailed quantitative study of 1, 2-dichloroethane cracking to vinyl chloride by a gas chromatographic pyrolysis device. **Ind. Eng. Chem. Res.** 35: 931-937.

Incropera, F., Dewitt, D. 2002. **Fundamentals of Heat and Mass Transfer.** 5th ed. John Wiley & Sons, New York.

James, R.W., C.E. Wicks, R.E. Wilson and G.L. Rorrer. 2007. **Fundamentals of momentum, heat, and mass transfer.** 5th ed. John Wiley & Son, Inc.

Kaggerud, Torbjorn Herder. 2007. **Modeling an EDC Cracker Using Computational Fluid Dynamics (CFD).** Available Source: http://www.divaportal. org/smash/record.jsf?pid =diva2:348459.

Kitabatake, M. and T. Onouchi. 1962. **Studies on the pyrolysis of organic chlorides.** Available Source: http: //kinetics .nist.gov /kinetics /index .jsp

Masoumi, M.E., Sadrameli, S.M., Towfighi, J., Niaei, A. 2006. Simulation, optimization and control of a thermal cracking furnace. **Energy.** 31: 516-527.

Mercado, E.R.L., Nunhez, J.R. 2000. **Modelagem do aquecimento de fluidos com escoamento em tubos.** Available Source: http://www.bibliotecadigital. unicamp.br/document/?code=vtls000197788.

Moghadam, A. A., I. Aksikas, S. Dubljevic and J.F. Forbes. 2013. Boundary optimal (LQ) control of coupled hyperbolic PDEs and ODEs. **Automatica.** 2: 526-533.

Occidental Petroleum Corporation. 2008. **Cracking EDC.** Available Source: http:// www.oxy.com/Our_Businesses/chemicals/Pages/chem_licensing_edc.aspx.

Panjapornpon, C., Limpanachaipornkul, P., Charinpanitkul, T. 2012. Control of coupled PDEs–ODEs using input–output linearization: Application to a cracking furnace. **Chem. Eng. Sci.** 75: 144-151.

Perry, R.H. and D.W. Green. 1997. **Perry's chemical engineers' handbook.** 7th ed. The McGraw-Hill Companies, Inc.

Rani, Y. and S.C. Patwardhan. 2007. Data-driven model based control of a multi-product semi-batch polymerization reactor. **Chem. Eng. Res. Des.** 85: 1397-1406.

Shahrokhi, M. and A. Nejati. 2002. Optimal Temperature control of a Propane thermal cracking reactor. **Ind. Eng. Chem. Res.** 41: 6572-6578.

Shang,H., J.F. Forbesand M.Guay. 2005. Feedback control of hyperbolic distributed parameter systems. **Chem. Eng. Sci.** 60: 969-980.

Van Geem, K.M., Heynderickx, G.J., Marin, G.B. 2004. Effect of radial temperature profiles on yields in steam cracking. **AIChE J.** 50: 173-183.

Warren, L.M., J.C. Smith and P. Harrirott. 2005. **Unit operations of chemical engineering.** 7th ed. The McGraw-Hill Companies, Inc.

Zeybek, Z. 2006. Role of adaptive heuristic criticism in cascade temperature control of an industrial tubular furnace. **Appl. Therm. Eng.** 26: 152-160.

Zychlinski, W. 1990. Coke formation in thermal decomposition of 1,2-dichloroethane-conclusions from radiotracer experiments. **Chem. Ing. Tech.** 42(8): 325.

APPENDICES

Appendix A

The model development of EDC cracking furnace

A Mathematical Model for the EDC Cracking Furnace

The full form of mass and energy balances, composing of the EDC concentration, gas temperature, tube temperature and furnace wall temperature dynamics, are neglected to formulate the mathematic model for EDC cracking furnace (Warren *et al*, 2005). The assumptions used in this model are shown as follows:

Assumptions

1) All gases in the system are ideal.

2) Only the heat of reaction in $C_2H_4Cl_2(g) \rightarrow C_2H_3Cl(g) + HCl(g)$ is concerned for the change of gas temperature.

3) Neglect effects of all elbows and fittings; straight tube is assumed.

4) The properties of gases in the tube are constant.

5) The tube temperature is varied along the z-direction only because of the pipe thickness << the coil distance.

6) The gas temperature and EDC concentration are varied in both the radius and distance of the coil.

Mass balance:

$$\frac{\partial C_{EDC}}{\partial t} + v_r \frac{\partial C_{EDC}}{\partial t} + \frac{v_\theta}{r}\frac{\partial C_{EDC}}{\partial \theta} + v_z \frac{\partial C_{EDC}}{\partial z} = \frac{k_g}{\rho_g C_{pg}}\left(\frac{1}{r}\frac{\partial}{\partial r}(r\frac{\partial C_{EDC}}{\partial r}) + \frac{1}{r^2}\frac{\partial^2 C_{EDC}}{\partial \theta^2} + \frac{\partial^2 C_{EDC}}{\partial z^2}\right) + r_{EDC} \quad \text{(A.1)}$$

With the assumptions above, the mass equation of EDC concentration is reduced to

$$\frac{\partial C_{EDC}}{\partial t} + v_z \frac{\partial C_{EDC}}{\partial z} = \frac{k_g}{\rho_g C_{pg}}\left(\frac{1}{r}\frac{\partial}{\partial r}(r\frac{\partial C_{EDC}}{\partial r})\right) + r_{EDC} \quad \text{(A.2)}$$

where r_{EDC} is the reaction rate which is $r_{EDC} = -k_0 C_{EDC} e^{\frac{-Ea}{RT_g}}$.

Thus, the EDC concentration model becomes

$$\frac{\partial C_{EDC}}{\partial t} = -v_z \frac{\partial C_{EDC}}{\partial z} + \frac{k_g}{\rho_g C_{pg}} \left(\frac{1}{r} \frac{\partial}{\partial r} (r \frac{\partial C_{EDC}}{\partial r}) \right) - k_0 C_{EDC} e^{\frac{-Ea}{RT_g}} \tag{A.3}$$

subjected to the initial and boundary equations:

$$B.C. \begin{cases} \frac{\partial C_{EDC}}{\partial r}(0, z, t) = 0 \\ \frac{\partial C_{EDC}}{\partial r}(R_i, z, t) = 0 \qquad I.C. \quad x_{p1}(r, z, 0) = x_{p1,0}(r, z) \\ C_{EDC}(r, 0, t) = C_{EDC,0} \end{cases} \tag{A.4}$$

Energy balance:

$$\rho c_p \left[\frac{\partial T}{\partial t} + v_r \frac{\partial T}{\partial r} + \frac{v_\theta}{r} \frac{\partial T}{\partial \theta} + v_z \frac{\partial T}{\partial z} \right] = k \left(\frac{1}{r} \frac{\partial}{\partial r} \left(r \frac{\partial T}{\partial r} \right) + \frac{1}{r^2} \frac{\partial^2 T}{\partial \theta^2} + \frac{\partial^2 T}{\partial z^2} \right) + \phi_v \tag{A.5}$$

- Energy balance in the gas temperature

According to the assumptions, the gas temperature dynamic is interested in the *r* and *z* directions, so Equation (A.5) becomes

$$\rho_g c_p \left[\frac{\partial T_g}{\partial t} + v_z \frac{\partial T_g}{\partial z} \right] = k_g \left(\frac{1}{r} \frac{\partial}{\partial r} \left(r \frac{\partial T}{\partial r} \right) + \frac{1}{r^2} \frac{\partial^2 T}{\partial \theta^2} + \frac{\partial^2 T}{\partial z^2} \right) + \phi_v \tag{A.6}$$

where ϕ_v is the external energy or the heat of reaction.

In this case, ϕ_v is the energy from the radiation effect from tube sent to the gas, and heat of reaction shown in Equation (A.7).

$$\phi_v = \frac{A_t F \sigma}{V_t}(T_t^4 - T_g^4) + \frac{|r_{EDC}'''|(\Delta H)_{EDC}}{\rho_g C_{p_g}} \tag{A.7}$$

From putting ϕ_v from Equation (A.7) in Equation (A.6) and rearranging, the dynamic of gas temperature will be received:

$$\frac{\partial T_g}{\partial t} = -v\frac{\partial T_g}{\partial z} + \frac{k_g}{\rho_g C_{p_g}}\frac{1}{r}\frac{\partial}{\partial r}\left(r\frac{\partial T_g}{\partial r}\right) + \frac{A_t F \sigma}{V_t \rho_g C_{pg}}(T_t^4 - T_g^4) + \frac{|r_{EDC}'''|(\Delta H)_{EDC}}{\rho_g C_{p_g}} \tag{A.8}$$

$$r_{EDC} = -k_0 C_{EDC} e^{-\frac{E_a}{RT_g}}$$

The dynamic of gas temperature in Equation (A.8) is subjected to the initial and boundary equations below.

$$B.C. \begin{cases} \dfrac{\partial T_g}{\partial r}(0,z,t) = 0 \\ T_g(R_i,z,t) = T_t(z,t) \\ T_g(r,0,t) = T_{g,0} \end{cases} \qquad I.C.\ \ T_g(r,z,t=0) = T_{g,0} \tag{A.9}$$

- Energy balance in the tube temperature

According to the assumptions, the tube temperature dynamic only pays attention to the diffusion effect in *z* direction, so Equation (A.5) becomes

$$\rho_t c_{p_t}\frac{\partial T_t}{\partial t} = k_t\frac{\partial^2 T_t}{\partial z^2} + \Phi_v \tag{A.10}$$

where ϕ_v is the external energy or the heat of reaction.

For the tube temperature balance, ϕ_v is the energy receiving from the radiation effect of the furnace wall, the radiation effect passing to the gas inside the coil, and the convection effect losing with fuel flow between the tube and furnace wall:

$$\phi_v = \frac{1}{V_{th,t}}\left[A_w F\sigma(T_w^4 - T_t^4) - A_i F\sigma(T_t^4 - T_g^4) - \frac{2\pi L}{\frac{\ln(R_o / R_i)}{k_t} + \frac{1}{R_o h_f}}(T_w - T_t)\right] \quad \text{(A.11)}$$

Then, put ϕ_v from Equation (A.11) in Equation (A.10) and rearrange it to be the dynamic of tube temperature as shown in Equation (A.12).

$$\frac{dT_t}{dt} = \frac{1}{\rho_t c_{p,t}} k_t \frac{\partial^2 T_t}{\partial z^2} + \frac{1}{\rho_t c_{p,t} V_{th,t}}\left[A_w F\sigma(T_w^4 - T_t^4) - A_i F\sigma(T_t^4 - T_g^4) - \frac{2\pi L}{\frac{\ln(R_o / R_i)}{k_t} + \frac{1}{R_o h_f}}(T_w - T_t)\right] \quad \text{(A.12)}$$

The dynamic of tube temperature in Equation (A.12) is subjected to the initial and boundary equations as follow:

$$B.C. \begin{cases} T_t(0,t) = T_{t,0} \\ \dfrac{\partial T_t}{\partial z}(L,t) = 0 \end{cases} \qquad I.C. \quad T_t(z,0) = T_{t,0} \quad \text{(A.13)}$$

- Energy balance in the furnace wall temperature

From the assumptions above, the furnace wall temperature only pays attention to the diffusion effect in *z* direction, so Equation (A.5) will be reduced to

$$m_w c_{p_w} \frac{\partial T_w}{\partial t} = \phi_v \quad \text{(A.14)}$$

where ϕ_v is the external energy or the heat of reaction.

For the furnace wall temperature balance, ϕ_v is the energy receiving from heat of combustion of fuel gas and the energy passed to the tube inside by radiation effect shown as follows:

$$\phi_v = \dot{m}_{fuel}\Delta H_{comb} - \sigma F A_w (T_w^4 - T_t^4) \quad \text{(A.15)}$$

-

After that ϕ_v from Equation (A.15) is put in Equation (A.14), the dynamic of furnace wall temperature is received:

$$\frac{\partial T_w}{\partial t} = \frac{\dot{m}_{fuel}\Delta H_{comb} - \sigma F A_w (T_w^4 - T_t^4)}{m_w c_{p_w}} \quad \text{(A.16)}$$

The initial equation of the furnace wall temperature dynamic is represented below.

$$I.C. \qquad T_w(z,0) = T_{w,0} \quad \text{(A.17)}$$

Appendix B

The controller formulation for EDC cracking furnace

The controller formulation for EDC cracking furnace

For this work, the I/O linearization technique is used to develop a controller for EDC cracking furnace. The controller is divided into two structures: I/O controller, and Setpoint tracking calculator with I/O controller.

1. Input/Output linearization technique

1.1 I/O controller

The I/O controller is developed, based on system in Equation (18) at the center of the exit tube (*r=0, z=L*). The controlled variable (*y*) and manipulated variable (*u*), in this system, are T_{gsp} and $\dot{m}_f$, respectively. The block diagram for such controller is shown in Appendix Figure 8.

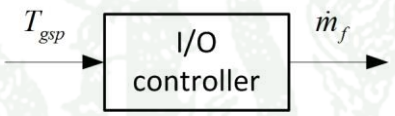

Appendix Figure B1 single I/O controller structure

The closed-loop response of the outlet gas temperature is requested in the form of

$$\left(\beta D+1\right)^3 T_g(z,t)\Big|_{r=0,z=L} = T_{gsp} \tag{B.1}$$

where D is a differential operator (i.e. $D \triangleq d/dt$), $T_g(z,t)\Big|_{r=0,z=L}$ is the gas temperature measured at the center of the exit tube, T_{gsp} is the setpoint of the gas temperature, and β is the tuning parameter that sets the speed of the response for the output T_g. Then, Equation (18) is substituted in Equation (B.1) to receive the controller equation as shown in Equation B.2.

$$\dot{m}_f = f(T_g, T_t, T_w, C_{edc}, \frac{\partial T_g}{\partial z}, \frac{\partial C_{edc}}{\partial z}, \frac{\partial^2 T_g}{\partial r^2}, \frac{\partial^2 C_{edc}}{\partial r^2}, \frac{\partial^2 T_t}{\partial z^2}) \quad \text{(B.2)}$$

In Equation (B.2), mass fuel flow is not expanded because it is very long and complex; it is about 8 times of Equation (B.6).

1.2 I/O controller with the setpoint tracking calculator

In this part, the I/O linearization technique is applied for the setpoint tracking calculator connected with I/O controller by basing on Equations 18 and 20. The controller equations are developed, based on the center of the exit tube (*r=0, z=L*). The controlled variable (*y*) and manipulated variable (*u*) of the setpoint tracking calculator and I/O controller in Figure 9 are T_{gsp}, v, and $\dot{m}_f$, respectively.

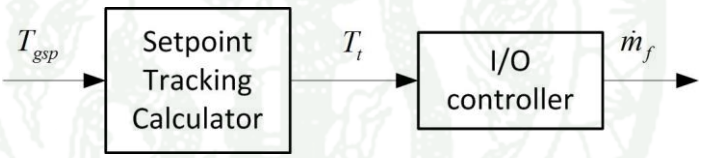

Appendix Figure B2 A coupling of setpoint tracking calculator and I/O controller structure

The closed-loop response of the outlet gas temperature and tube temperature are requested in Equations (B.3) and (B.4) respectively.

$$(\varepsilon D+1)\ T_g(z,t)\big|_{r=0,z=L} = T_{gsp} \quad \text{(B.3)}$$

$$(\beta D+1)^2\ T_t(z,t)\big|_{z=L} = T_{tsp} \quad \text{(B.4)}$$

where *D* is a differential operator (i.e. $D \triangleq d/dt$), $T_g(z,t)\big|_{r=0,z=L}$ is the gas temperature measured at the center of the exit tube, T_{gsp} is the setpoint of the gas temperature, ε is

the tuning parameter that sets the speed of the response for the output T_g , and β is the tuning parameter that sets the speed of the response for the output T_t.

Then, Equations (18) and (20) are respectively substituted in Equations (B.3) and (B.4) to receive the controller equations as follow.

$$T_{tsp} = (-\beta_1 k_g T_g V_t + C_{pg}\rho_g T_{gsp} V_t + \beta_1 C_{pg}\rho_g \frac{\partial T_g}{\partial z} v V_t + (\beta_1 \Delta H k_0 V_t C_{edc}) / exp(Ea / (RT_g)) - C_{pg}\rho_g V_t T_g + A_i \beta_1 F \sigma T_g^{\,4})^{(1/4)} / (A_i \beta_1 F \sigma)^{(1/4)} \quad \text{(B.5)}$$

$$\dot{m}_f = (1/(4A_w\beta_2^2 \Delta H_{com} F \sigma T_w^{\,3})) * (C_{pt} C_{pw} m_t m_w (T_{tsp} - T_t + (4A_w^{\,2}\beta_2^2 F^2 \sigma^2 T_w^3 (-T_t^{\,4} + T_w^4)) / (C_{pt} C_{pw} m_t m_w) - (4A_w \beta_2^2 F \sigma T_t^{\,3} ((-k_t) m_t T_t - A_i \rho_t F \sigma T_g^{\,4} + A_i \rho_t F \sigma T_t^4 + A_w \rho_t F \sigma T_t^4 - A_w \rho_t F \sigma T_w^4)) / (C_{pt}^{\,2} \rho_t m_t^{\,2}) - (2\beta_2 (k_t m_t T_t + A_i \rho_t F \sigma T_g^{\,4} - A_i \rho_t F \sigma T_t^4 - A_w \rho_t F \sigma T_t^4 + A_w \rho_t F \sigma T_w^{\,4})) / (C_{pt} \rho_t m_t) + (1/(C_{pg} C_{pt}^{\,2} \rho_g \rho_t m_t^{\,2} V_t))((4A_i \beta_2^2 F \sigma((-C_{pt})\rho_t exp(E_a / (RT_g)) k_g m_t \partial^2 T_g / \partial r^2 V_t T_g^{\,3} + C_{pg} C_{pt} \rho_g \rho_t exp(E_a / (RT_g)) m_t \partial T_g / \partial z V_t T_g^{\,3} + C_{pt} \Delta H_{com} \rho_t k m_t V_t C_{edc} T_g^{\,3} + A_i C_{pt} \rho_t exp(E_a / (RT_g)) F m_t \sigma T_g^{\,7} + C_{pg} \rho_g exp(E_a / (RT_g)) k_t m_t \partial^2 T_g / \partial z^2 V_t T_t^3 + A_i C_{pg} \rho_g \rho_t exp(E_a / (RT_g)) F \sigma V_t T_g^{\,4} T_t A_i C_{pg} \rho_g \rho_t exp(E_a / (RT_g)) F \sigma V_t T_t^{\,7} - A_w C_{pg} \rho_g \rho_t exp(E_a / (RT_g)) F \sigma V_t T_t^{\,7} + A_w C_{pg} \rho_g \rho_t exp(E_a / (RT_g)) F \sigma V_t T_t^3 T_w^4)) / exp(E_a / (RT_g))))) \quad \text{(B.6)}$$

CURRICULUM VITAE

NAME : Mr. Chawin Taweerojkulsri

BIRTH DATE : November 18, 1989

BIRTH PLACE : Bangkok, Thailand

EDUCATION :

YEAR	**INSTITUTE**	**DEGREE/DIPLOMA**
2012	Kasetsart Univ.	B.Eng. (Chemical Engineering)

POSITION/TITLE : Student

WORK PLACE : Faculty of Engineering, Kasetsart University

SCHOLARSHIP/AWARDS : the Center of Excellence on Petrochemicals and Materials Technology (PETROMAT)